Electronic Supplementary Information for

TBAF-Catalyzed Inverse Vulcanization under Mild Conditions Enabling Synthesis of Refractive Indexing, Ultraviolet Blocking and Light Transmiting Sulfur-Rich Polymers

Xing-Rui Cao,[a] Xiao-Jun Liu,[a] Wei-Ping Li,[c] Dong-Ping Chen,*[a] Tom Hasell,[b] Xiaofeng Wu,[b] Xi-Cun Wang,*[a] and Zheng-Jun Quan,*[a]

[a.] College of Chemistry and Chemical Engineering, Northwest Normal University, Lanzhou 730070, Gansu, China

[b.] Materials Innovation Factory, and Department of Chemistry, University of Liverpool, Liverpool, UK L69 7ZD

[c.] Gansu Research Institute of Chemical Industry Co.,Ltd.

**Corresponding author: D. -P. Chen (E–mail: chendp@nwnu.edu.cn)*

X. F. Wu (E–mail: xfwu@liverpool.ac.uk)

X.-C. Wang (E–mail: wangxicun@nwnu.edu.cn)

Z.-J. Quan (E–mail: quanzhengjun@hotmail.com)

Table of Contents

1. Materials and instrumentation

Materials

Sulfur (S_8, sublimed, ≥ 99.5%, Sigma-Aldrich), 1,3-Diisopropenylbenzene (DIB, >97.0%, Shanghai Aladdin Biochemical Technology Co. Ltd., China), Ethylene glycol dimethacrylate (EGDMA, >95.0%, Aldrich), Acrylamide (AA, >99.0%, Energyseal, Sigma-Aldrich), Trimethylolpropane triacrylate, (TMPTA,＞95%, Sigma-Aldrich), 1,3,5-triacryloylhexahydro-1,3,5-triazine (TAT 99.0%, Energyseal, Sigma-Aldrich), Benzyl Methacrylate (PBzMA, 98.0%, Aldrich), (STEGMA, 97.0%, Macklin), Butyl Methacrylate (BMA, AR, ≥ 99.0% (GC), Energyseal, Sigma-Aldrich), *N,N′*-methylene diacrylamide (MBA, 99.0%, Energyseal, Sigma-Aldrich), Styrene (St, 99.5%, stabilized with TBC, Energyseal, Sigma-Aldrich), Polyethylene glycol diacrylate (PEG, M.W.200, Energyseal, Sigma-Aldrich), 1,3-Diisopropenylbenzene (DIB, >97.0%, Aladdin), Myrcene (Mye, >90.0%, Aladdin)，1,3-Divinylbenzene (DVB, >80.0%, Aldrich), 1-Octene (1-OC, 98%,Aladdin), Tetrabutylammonium fluoride (TBAF, 1.0mol/L in THF, Energyseal, Sigma-Aldrich), Tetrabutylammonium fluoride trihydrate (TBAF, 98%, Energyseal, Sigma-Aldrich), Tetrabutylammonium bromide (TBABr, 99%, Energyseal, Sigma-Aldrich), Tetrabutylammonium iodide (TBAI, 98%, Energyseal, Sigma-Aldrich), Tetrabutylammonium chloride (TBACl, 98%, Energyseal, Sigma-Aldrich), Potassium fluoride (KF, anhydrous, 99%, Energyseal, Sigma-Aldrich), Caesium fluoride (CsF, 99.5%(metals basis), Energyseal, Sigma-Aldrich), Sodium fluoride (NaF, 98%, Energyseal, Sigma-Aldrich), Chloroform-d ($CDCl_3$, 99.8 atom%D, stab.mit Ag, cont.0.03V/V% TMS, Ningbo Cuiying Chemical Technology Co., Ltd), Tetrahydrofuran (THF, 99.5%, Extra Dry, with molecular sieves, stabilized with BHT, Water≤50ppm (by K.F.), Energyseal, Sigma-Aldrich).

Instrumentation

Nuclear Magnetic Resonance (NMR, Varian Mercury Plus 400 and Agilent DD2-600 MHz, USA) provides detailed information about molecular structure and chemical reactions processes. Fourier-Transform Infrared (FT-IR, Digilab FTS-3000, USA)

spectra exhibit the changes in chemical bonds before and after polymerization. Differential Scanning Calorimetry (DSC, TAQ2000, USA) was conducted at constant heating and cooling rates of 5 ℃ min^{-1} under N_2 atmosphere in the range from -50 ℃ to 150 ℃. Thermogravimetric Analysis (TGA, Mettler Toledo TGA/DSC1, Switzerland) was performed in a N_2 flow from 25 to 800 ℃ at a rate of 10 ℃ min^{-1}. X-ray photoelectron spectroscopy (XPS, Thermo ESCALAB 250XI). Gel permeation chromatography (GPC, PL-GPC50, USA). HPLC grade N, N-dimethylformamide (DMF) was used as an eluent at a flow rate of 1 mL/min. The number-average molecular weight and polydispersity (Mw/Mn) data are reported relative to polystyrene standards. XPS was performed using a Thermo ESCALAB with a monochromatic Al Kα X-ray source having an energy of 1486.6 eV. Powder X-ray Diffraction (PXRD, Rigaku D/Max-2200PC, Japan) patterns of S_8, polymers and composites were characterized using Cu Kα radiation (λ=1.5418 Å) at 40 kV, 100 mA, scanning range was from 5° to 80°. Uvisel plus Elliptical polarization spectroscopy is a non-destructive and non-contact optical measurement technology. Based on measuring the change in polarization state of linearly polarized light after reflection by a film sample, the thickness and optical properties of the film, interface and surface roughness layer are obtained through model fitting. Set the wavelength range to 500-1600 nm, and take 4 points in this range to test the refractive index, such as 600 nm, 800 nm, 1100 nm, and 1500 nm.

$Pb(OAc)_2$ test paper was used to detect H_2S under different reaction conditions.

2. Experimental section

a. General procedure for TBAF-catalyzed IV polymerization for synthesizing sulfur polymers at r.t.

To a 20 mL glass vial with magnetic stir bar was added sulfur (S_8, 200 mg, 0.78 mmol) and added TBAF (5%, 20 mg), after sealing it, three consecutive argon replacements were performed. EGDMA (200 mg) and THF (0.5 mL, 6.15 mmol) was then added to the straight tube via syringe. The reaction mixture was stirred at room temperature (r.t.) until the reaction mixture caused the stirrer bar to cease motion (2-18 h) to obtain the crude product. The crude product was subsequently placed in a 60 °C

oven for drying, removed for yield calculation and characterized by FTIR, NMR and XRD. Alternatively, the crude product was washed with CS_2、H_2O、EtOH and dried to give the desired P(S-EGDMA) for further instrumentations. Other IV polymers were prepared according to the above method by using crosslinkers, such as MBA, TMPTA, STEGMA, AA, TAT, PBzMA, BMA, and PEG.

b. General procedure for the preparation of Poly(S-EGDMA-MBA) with 50-wt% EGDMA and 50-wt% MBA.

To a 20 mL glass vial with magnetic stir bar was added sulfur (S_8, 200 mg, 0.78 mmol) and added TBAF (5%, 30 mg), after sealing it, three consecutive argon replacements were performed. Ethylene glycol dimethacrylate (EGDMA, 200 mg, 1.01 mmol) and *N,N′*-methylene diacrylamide (MBA, 200 mg, 1.30 mmol) and THF (0.5 mL, 6.15 mmol) was then added immediately to the straight tube via syringe. The reaction mixture was stirred at room temperature (r.t.) until the reaction mixture caused the stirrer bar to cease motion (18 h). The product was then taken directly from the vial to obtain the crude product. It was subsequently placed in a 60°C oven for drying, removed for yield calculation and characterized by FTIR, NMR and XRD. Alternatively, the crude product was washed with CS_2、H_2O、EtOH and dried to give the desired P(S-EGDMA-MBA) for further property characterization, including DSC, TG, Index, GPC and UV resistance.

c. General procedure for TBAF-catalyzed IV polymerization for synthesizing sulfur polymers at 80℃.

To a 20 mL glass vial with magnetic stir bar was added sulfur (S_8, 200 mg, 0.78 mmol) and added TBAF (5%, 20 mg), after sealing it, three consecutive argon replacements were performed. DIB (200 mg) and THF (0.5 mL, 6.15 mmol) was then added to the straight tube via syringe. The reaction mixture was stirred at 80℃ until the reaction mixture caused the stirrer bar to cease motion (2-18 h) to obtain the crude product. The crude product was subsequently placed in a 60 °C oven for drying, removed for yield calculation and characterized by FTIR, NMR and XRD. Alternatively, the crude product was washed with CS_2、H_2O、EtOH and dried to give the desired P(S-

DIB) for further instrumentations. Other IV polymers were prepared according to the above method by using crosslinkers, such as DVB, St, MYE and 1-OC.

Preparation of poly(S-EGDMA-MBA) films

Poly(S-EGDMA-MBA) films were prepared by a tablet press and pressing (10 MPa) at 25 ℃ for 2 min. Broken pieces of poly(S_8-EGDMA-MBA) films were gathered and reprocessed to the original form using the same procedure.

3. Screening of catalysts for inverse vulcanization of sulfur and EGDMA

Table S1 Screening of conditions for inverse vulcanization of sulfur with EGDMA[a]

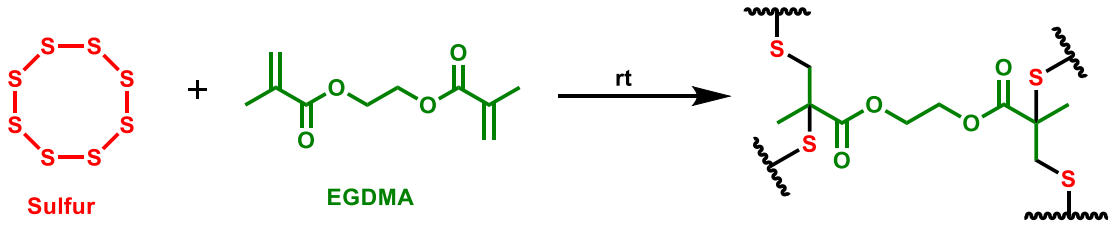

Entry	Catalyst	Solvent	Yield(%)
1	TBAF	THF	89
2	TBACl	THF	--[b]
3	TBAI	THF	--[b]
4	TBABr	THF	--[b]
5	CsF	THF	--[b]
6	NaF	THF	--[b]
7	KF	THF	--[b]
8	TBAF	MeCN	--[b]
9	TBAF	$CHCl_3$	--[b]

a The reaction was at r.t. for 12 h, with stirring. Weight ratio of cross-linker (EGDMA, 200 mg) and sulfur (200 mg) of 1:1 and 5 wt% catalyst loading.
b no polymers were obtained under any of the other conditions.

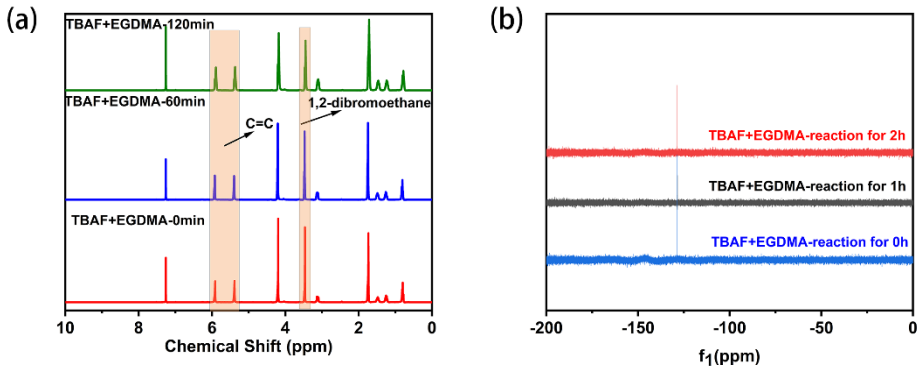

Fig. S1 (a) ^{1}H NMR (400 MHz) and (b) ^{19}F NMR spectrum comparison of 0 min、60 min、120 min in $CDCl_3$ at 25 °C.

4. FTIR spectrum of polymer (Figs. S2-S16)

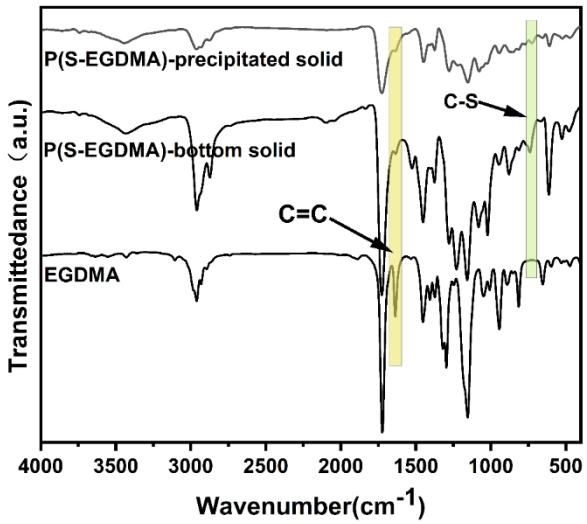

Fig. S2 FTIR spectrum of poly(S-EGDMA) catalyzed by TBAF.

Compared with the pristine EGDMA, the poly(S-EGDMA) shows that the peaks 3025 and 1639 cm^{-1} bands attributed to =C-H and $=CH_2$ are disappered. Poly(S-EGDMA) and the new peak at 746 cm^{-1} is attributed to C-S, which shows that poly(S-EGDMA) have been successfully prepared. Through the experiment we observed that the reaction process will appear in the glass tube wall yellow transparent material, through the FTIR, the wall and the bottom of the tube appeared the product FTIR spectrum is consistent.

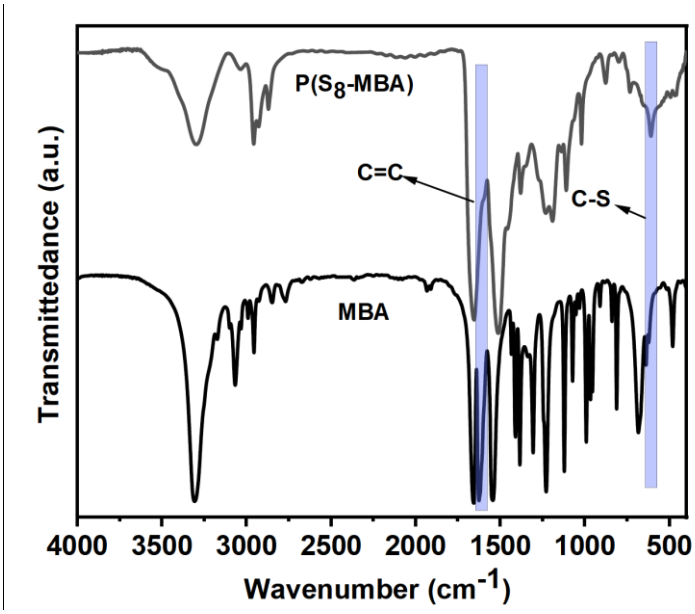

Fig. S3 FTIR spectrum of poly(S-MBA) catalyzed by TBAF.

Compared with the pristine MBA, the poly(S-MBA) shows that the peaks 3061 and 1627 cm^{-1} bands attributed to =C-H and $=CH_2$ are disappered. Poly(S-MBA) and the new peak at 608 cm^{-1} is attributed to C-S, which shows that poly(S-MBA) have been successfully prepared.

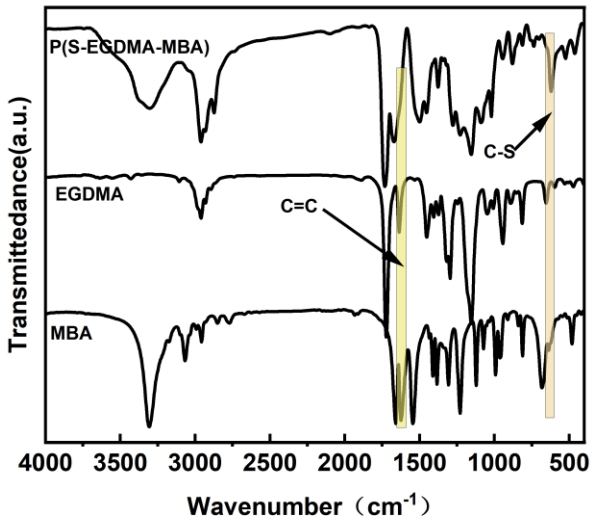

Fig. S4 FTIR spectrum of poly(S-EGDMA-MBA) catalyzed by TBAF.

Compared with the pristine EGDMA and MBA, the poly(S-EGDMA-MBA) shows that the peaks 3025, 3061 and 1639 cm^{-1},1627 cm^{-1} bands attributed to =C-H and $=CH_2$ are disappered. Poly(S-EGDMA-MBA) and the new peak at 617 cm^{-1} is attributed to C-S, which shows that poly(S-EGDMA-MBA) have been successfully prepared.

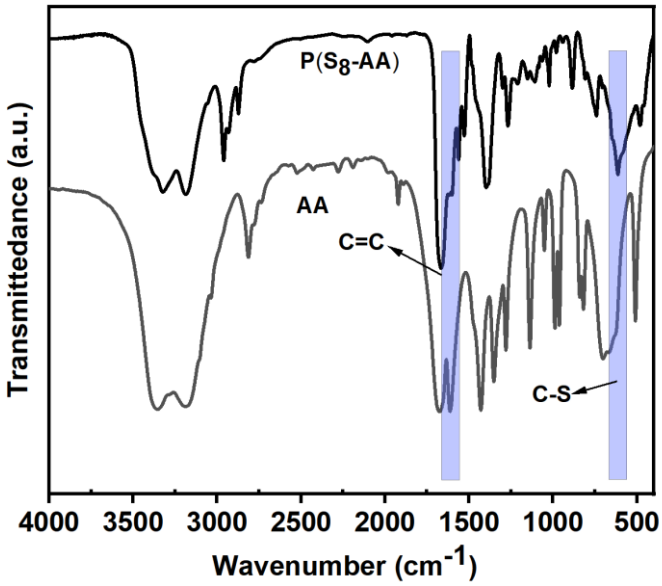

Fig. S5 FTIR spectrum of poly(S-AA) catalyzed by TBAF.

Compared with the pristine AA, the poly(S-AA) shows that the peaks 2964 and 1612 cm^{-1} bands attributed to =C-H and $=CH_2$ are disappered. Poly(S-AA) and the new peak at 609 cm^{-1} is attributed to C-S, which shows that poly(S-AA) have been successfully prepared.

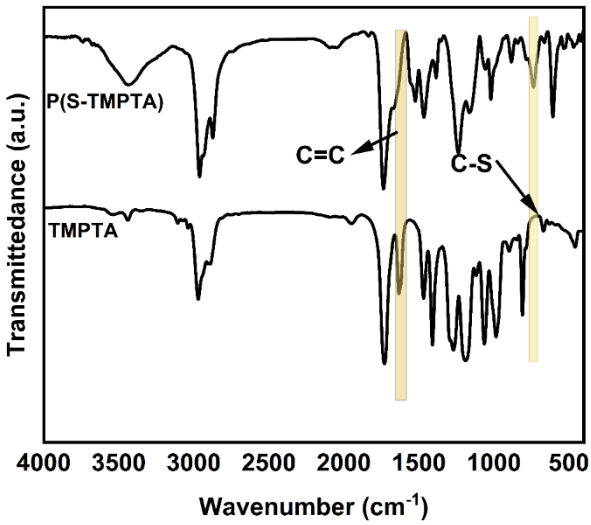

Fig. S6 FTIR spectrum of poly(S-TMPTA) catalyzed by TBAF.

Compared with the pristine TMPTA, the poly(S-TMPTA) shows that the peaks 2970 and 1635 cm^{-1} bands attributed to =C-H and $=CH_2$ are disappered. Poly(S-TMPTA) and the new peak at 732 cm^{-1} is attributed to C-S, which shows that poly(S-TMPTA) have been successfully prepare.

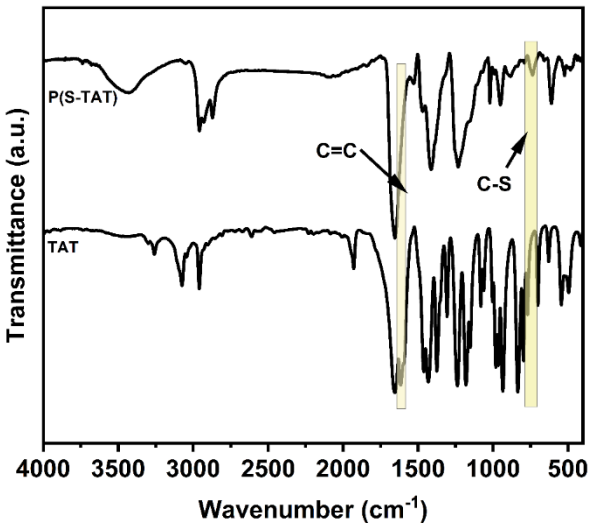

Fig. S7 FTIR spectrum of poly(S-TAT) catalyzed by TBAF.

Compared with the pristine TAT, the poly(S-TAT) shows that the peaks 2956 and 1616 cm^{-1} bands attributed to =C-H and $=CH_2$ are disappered. Poly(S-TAT) and the new peak at 731 cm^{-1} is attributed to C-S, which shows that poly(S-TAT) have been successfully prepared.

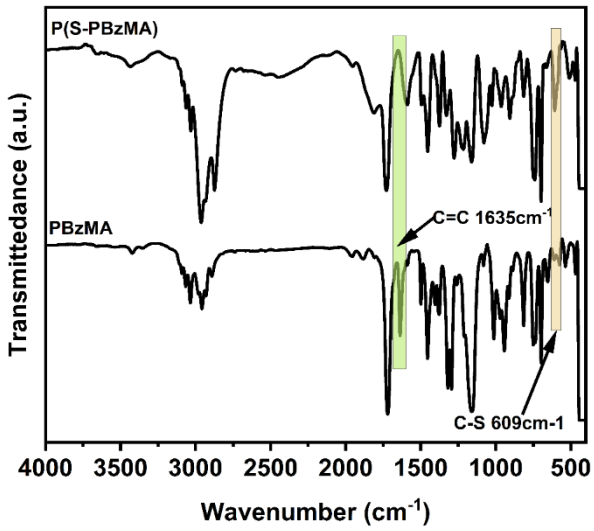

Fig. S8 FTIR spectrum of poly(S-PBzMA) catalyzed by TBAF.

Compared with the pristine PBzMA, the poly(S-PBzMA) shows that the peaks 2964 and 1635 cm^{-1} bands attributed to =C-H and $=CH_2$ are disappered. Poly(S-PBzMA) and the new peak at 609 cm^{-1} is attributed to C-S, which shows that poly(S-PBzMA) have been successfully prepared.

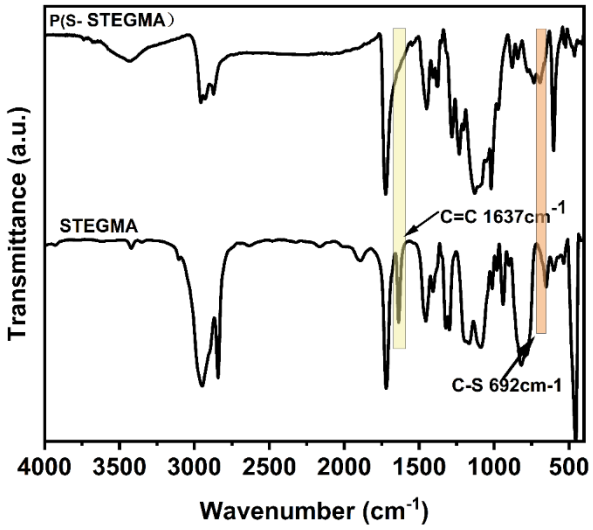

Fig. S9 FTIR spectrum of poly(S-STEGMA) catalyzed by TBAF.

Compared with the pristine STEGMA, the poly(S-STEGMA) shows that the peaks 2954 and 1637 cm^{-1} bands attributed to =C-H and $=CH_2$ are disappered. Poly(S-STEGMA) and the new peak at 692 cm^{-1} is attributed to C-S, which shows that poly(S-STEGMA) have been successfully prepared.

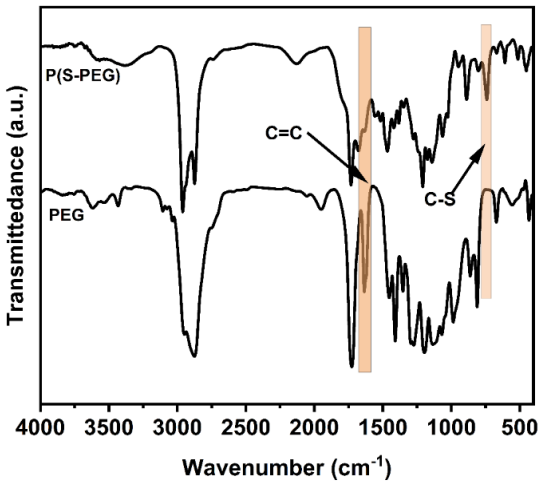

Fig. S10 FTIR spectrum of poly(S-PEG) catalyzed by TBAF.

Compared with the pristine PEG, the poly(S-PEG) shows that the peaks 2954 and 1631 cm^{-1} bands attributed to =C-H and $=CH_2$ are disappered. Poly(S-PEG) and the new peak at 742 cm^{-1} is attributed to C-S, which shows that poly(S-PEG) have been successfully prepared.

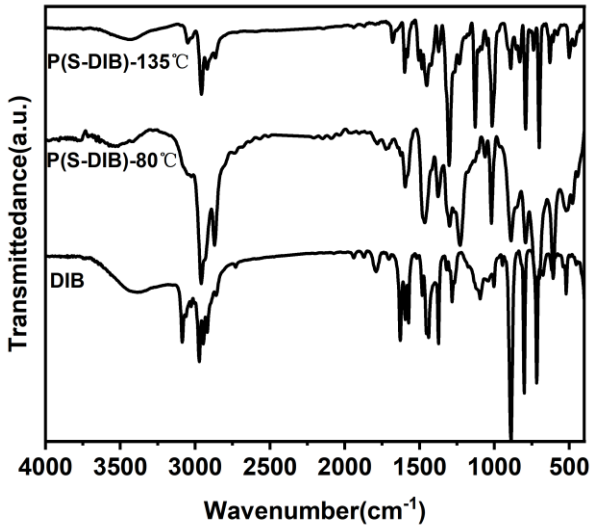

Fig. S11 FTIR spectrum of poly(S-DIB) catalyzed by TBAF.

Compared with the pristine DIB, the poly(S-DIB) shows that the peaks 3088 and 1629 cm^{-1} bands attributed to =C-H and $=CH_2$ are disappered. Poly(S-DIB) and the new peak at 1014 cm^{-1} is attributed to C-S, which shows that poly(S-DIB) have been successfully prepared.

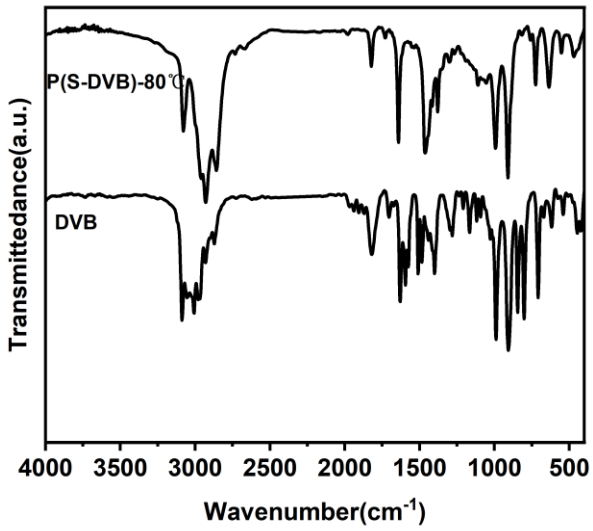

Fig. S12 FTIR spectrum of poly(S-DVB) catalyzed by TBAF.

Compared with the pristine DVB, the poly(S-DVB) shows that the peaks 3080 and 1629 cm^{-1} bands attributed to =C-H and $=CH_2$ are disappered. Poly(S-DVB) and the new peak at 725 cm^{-1} is attributed to C-S, which shows that poly(S-DVB) have been successfully prepared.

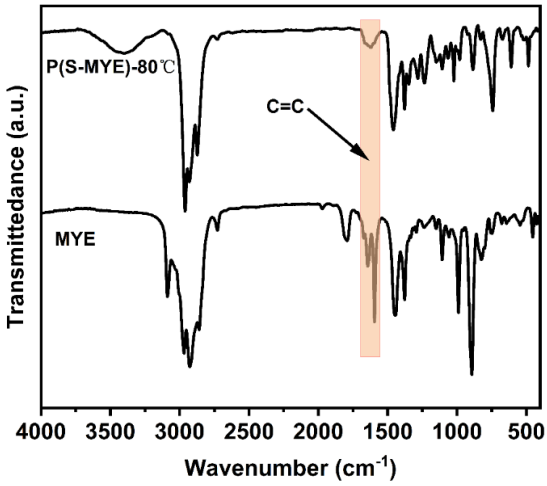

Fig. S13 FTIR spectrum of poly(S-MYE) catalyzed by TBAF.

Compared with the pristine MYE, the poly(S-MYE) shows that the peaks 3089 and 1595 cm^{-1} bands attributed to =C-H and $=CH_2$ are disappered. Poly(S-MYE) and the new peak at 607 cm^{-1} is attributed to C-S, which shows that poly(S-MYE) have been successfully prepared.

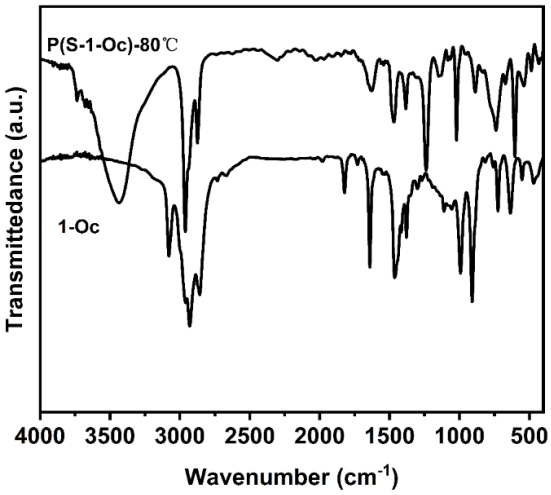

Fig. S14 FTIR spectrum of poly(S-1-OC) catalyzed by TBAF.

Compared with the pristine 1-OC, the poly(S-1-OC) shows that the peaks 3082 and 1643 cm^{-1} bands attributed to =C-H and $=CH_2$ are disappered. Poly(S-1-OC) and the new peak at 601 cm^{-1} is attributed to C-S, which shows that poly(S-1-OC) have been successfully prepared.

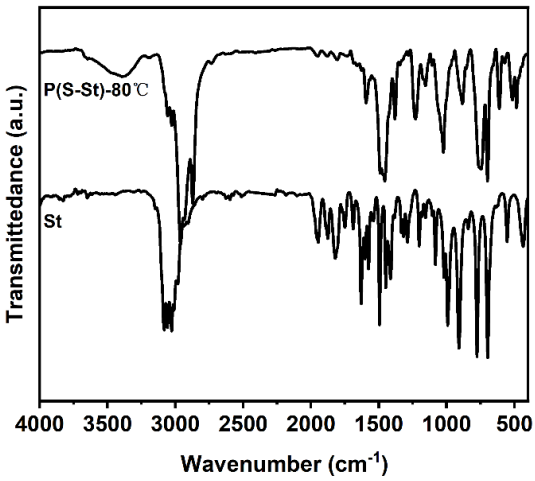

Fig. S15 FTIR spectrum of poly(S-St) catalyzed by TBAF.

Compared with the pristine St, the poly(S-St) shows that the peaks 3084 and 1631 cm^{-1} bands attributed to =C-H and $=CH_2$ are disappered. Poly(S-St) and the new peak at 609 cm^{-1} is attributed to C-S, which shows that poly(S-St) have been successfully prepared.

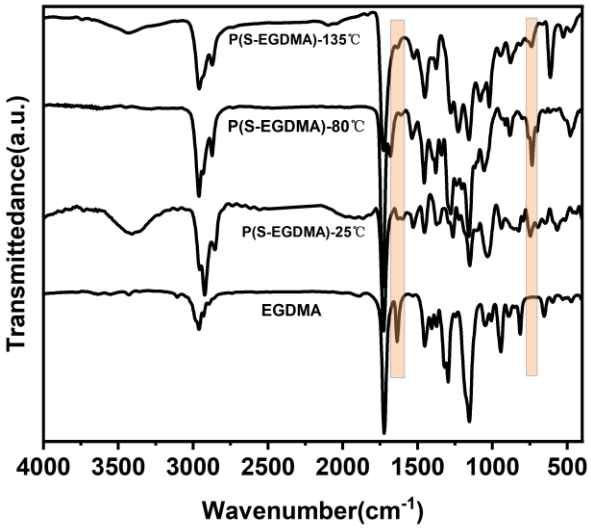

Fig. S16 FTIR spectrum of poly(S-EGDMA) catalyzed by TBAF.

Compared with the pristine EGDMA, the poly(S-EGDMA) shows that the peaks 3025 and 1639 cm^{-1} bands attributed to =C-H and $=CH_2$ are disappered. Poly(S-EGDMA) and the new peak at 709 cm^{-1} is attributed to C-S, which shows that poly(S-EGDMA) have been successfully prepared.

5. ^{1}H-NMR spectra of polymer (Figs. S16-S27)

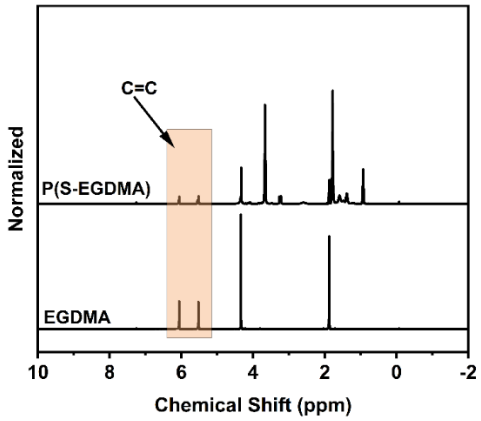

Fig. S17 ^{1}H-NMR spectra of EGDMA and the reaction system after introduction of TBAF and THF into EGDMA for 8 h at room temperature (r.t.) After 12 h of reaction, the polymer obtained was difficult to dissolve due to its high degree of cross-linking, so the viscous polymer obtained at 8 h was selected for ^{1}H NMR detection. Selection of $CDCl_3$ solvated polymers for ^{1}H NMR testing.

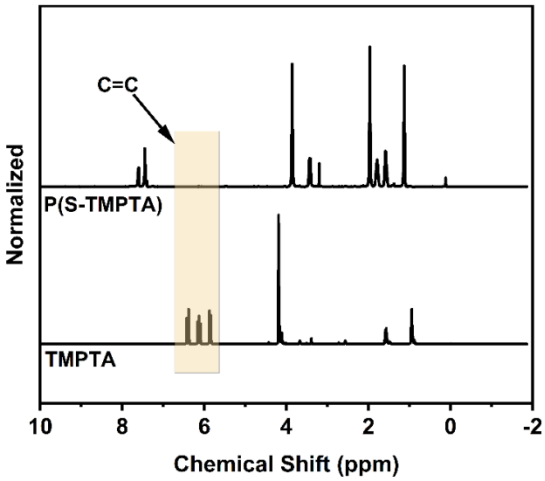

Fig. S18 ^{1}H-NMR spectra of TMPTA and the reaction system after introduction of TBAF and THF into TMPTA for 1 h at r.t. Selection of $CDCl_3$ solvated polymers for ^{1}H NMR testing.

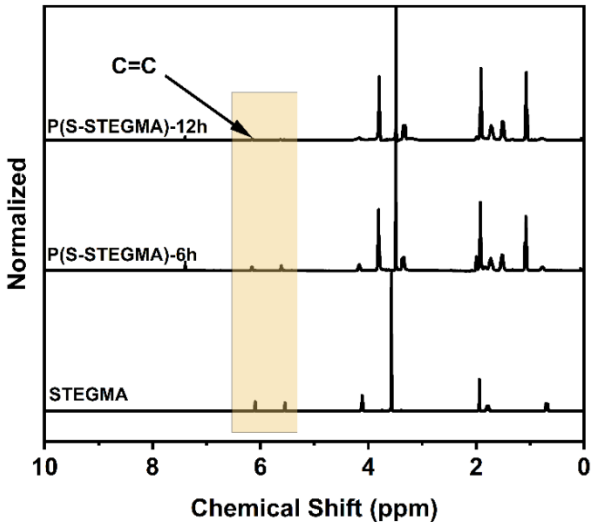

Fig. S19 ^{1}H-NMR spectra of STEGMA and the reaction system after introduction of TBAF and THF into STEGMA for 12 h at r.t. Selection of $CDCl_3$ solvated polymers for ^{1}H NMR testing.

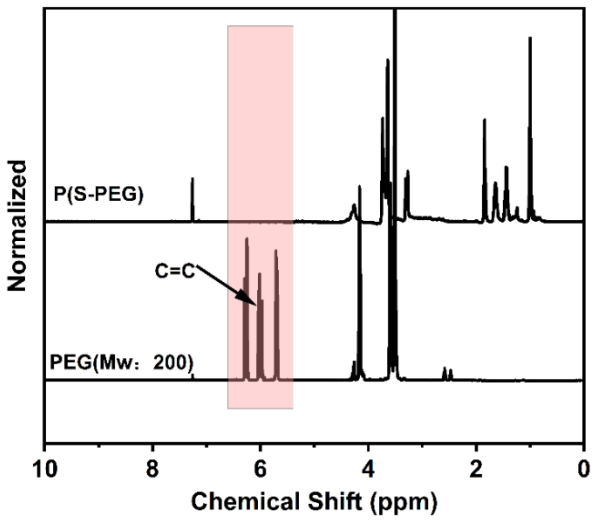

Fig. S20 ^{1}H-NMR spectra of PEG and the reaction system after introduction of TBAF and THF into PEG for 18 h at r.t. Selection of $CDCl_3$ solvated polymers for ^{1}H NMR testing.

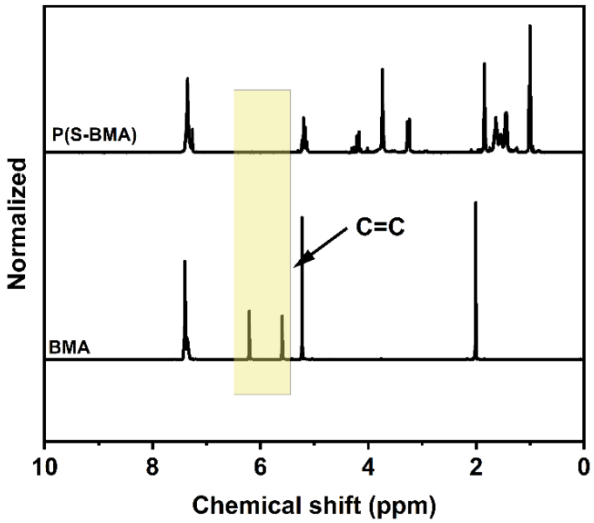

Fig. S21 ^{1}H-NMR spectra of BMA and the reaction system after introduction of TBAF and THF into BMA for 18 h at r.t. Selection of $CDCl_3$ solvated polymers for ^{1}H NMR testing.

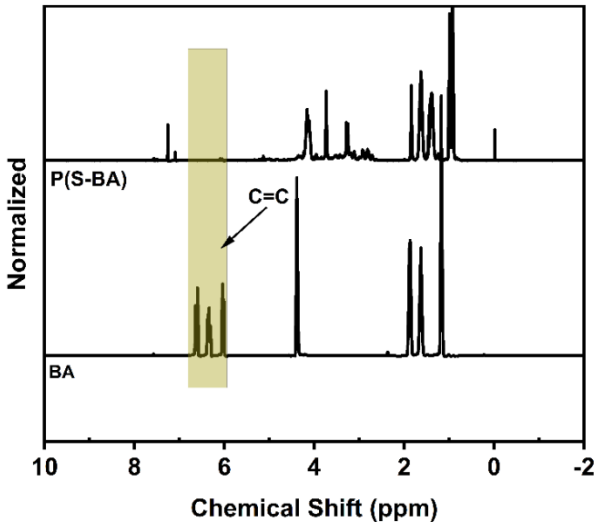

Fig. S22 ^{1}H-NMR spectra of BA and the reaction system after introduction of TBAF and THF into BA for 18 h at r.t. Selection of $CDCl_3$ solvated polymers for ^{1}H NMR testing.

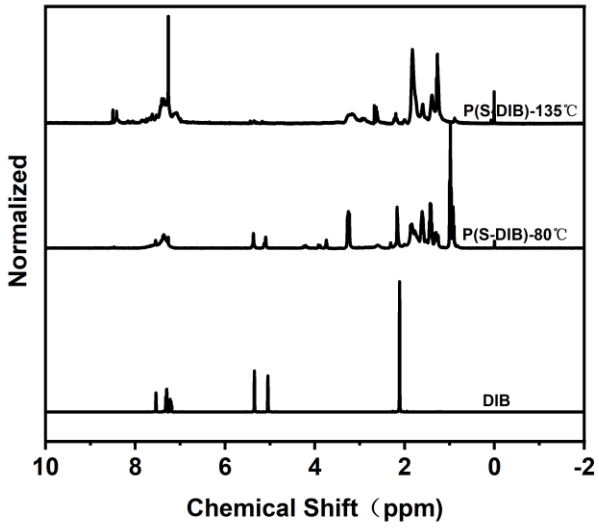

Fig. S23 ^{1}H-NMR spectra of DIB and the reaction system after introduction of TBAF and THF into DIB for 18 h at 80 ℃. Selection of $CDCl_3$ solvated polymers for ^{1}H NMR testing.

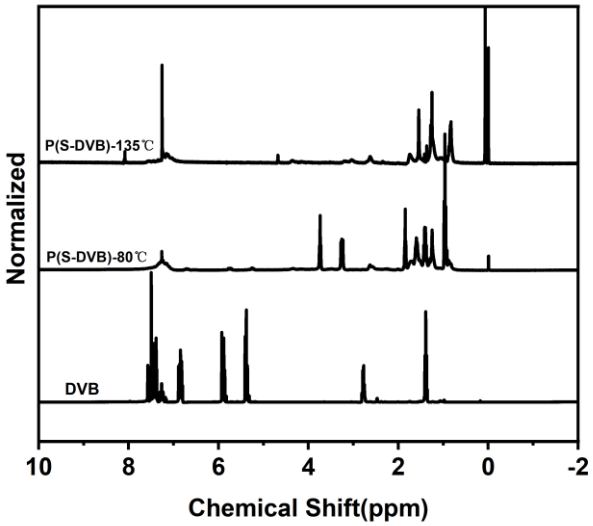

Fig. S24 ^{1}H-NMR spectra of DVB and the reaction system after introduction of TBAF and THF into DVB for 12 h at 80 ℃. Selection of $CDCl_3$ solvated polymers for ^{1}H NMR testing.

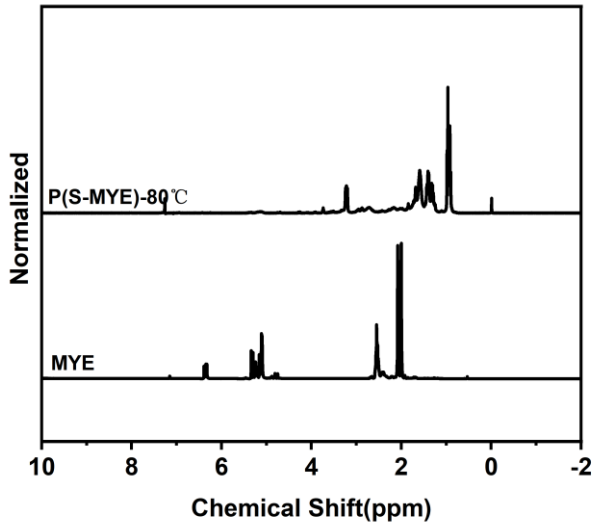

Fig. S25 ^{1}H-NMR spectra of MYE and the reaction system after introduction of TBAF and THF into MYE for 12 h at 80 ℃. Selection of $CDCl_3$ solvated polymers for ^{1}H NMR testing.

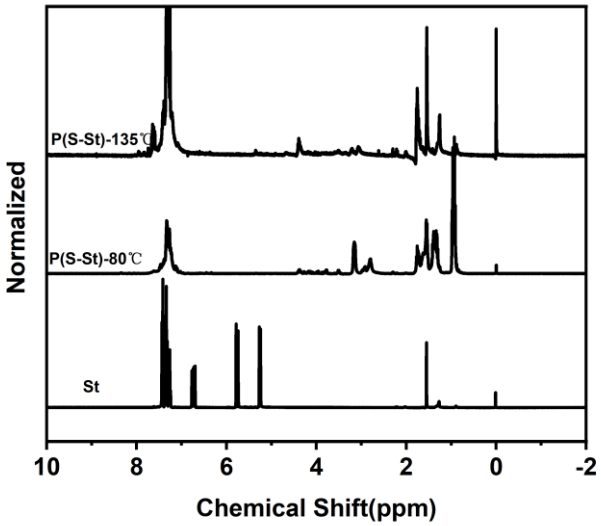

Fig. S26 ^{1}H-NMR spectra of St and the reaction system after introduction of TBAF and THF into St for 12 h at 80 ℃. Selection of $CDCl_3$ solvated polymers for ^{1}H NMR testing.

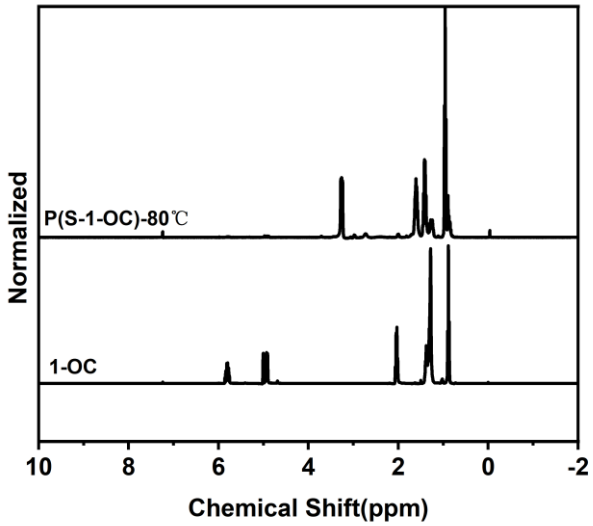

Fig. S27 ^{1}H-NMR spectra of 1-OC and the reaction system after introduction of TBAF and THF into 1-OC for 12 h at 80 ℃. Selection of $CDCl_3$ solvated polymers for ^{1}H NMR testing.

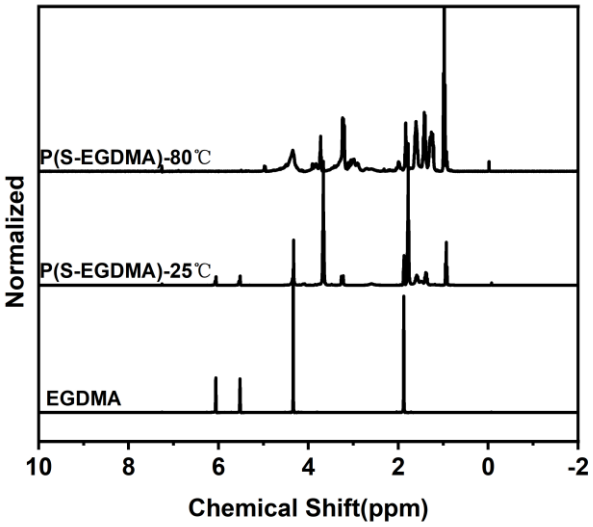

Fig. S28 ^{1}H-NMR spectra of EGDMA and the reaction system after introduction of TBAF and THF into EGDMA for 12 h at 80 ℃. Selection of $CDCl_3$ solvated polymers for ^{1}H NMR testing.

6. Preparation of copolymer P(S-EGDMAy-MBAz) and its properties

Fig. S29 P(S-EGDMA-MBA) obtained with different material ratios

After reacting the polymers at different material ratios for different periods of time, the polymers take on a transparent state that can be used to make optical lens materials by compression moulding. This is the picture after polymerization.

7. Structural characterization of P(S-EGDMA-MBA)

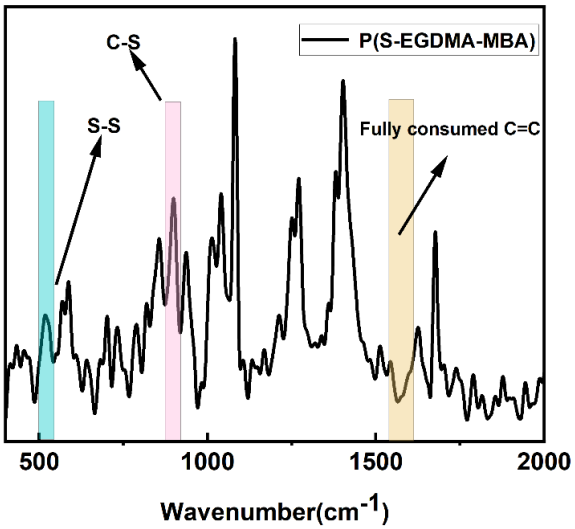

Fig. S30 Raman spectrum of poly(S-EGDMA-MBA).

The structure of the product was analyzed by Raman revealing that the symmetric/asymmetric stretching vibration at 495-525 cm^{-1} corresponds to S-S bonding, while the symmetric/asymmetric stretching vibration at 871-921 cm^{-1} is attributed to C-S bonding. The absence of absorption peaks at 1548-1610 cm^{-1} indicates the formation of sulfur adducts with an unsaturated double bond in the olefin, thereby confirming the successful preparation of the polymer.

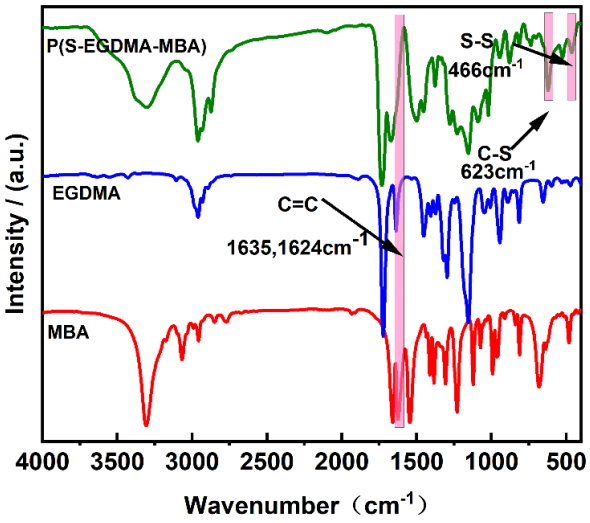

Fig. S31 FTIR spectrum of EGDMA, MBA and poly(S-EGDMA-MBA).

Fourier Transform Infrared Spectroscopy (FTIR) further confirmed the presence of stretching vibrations of S-S bond at 466 cm^{-1} and C-S bond at 623 cm^{-1}. Additionally, the disappearance of C=C peaks at 1624 cm^{-1} and 1635 cm^{-1} provided further evidence of the successful preparation of the copolymer. The conjugation effect of amide in MBA causes the C=O peak to exhibit characteristics of a partial single bond, resulting in a shift to a lower wave number, potentially nearing the absorption peak of unsaturated C=C in MBA.

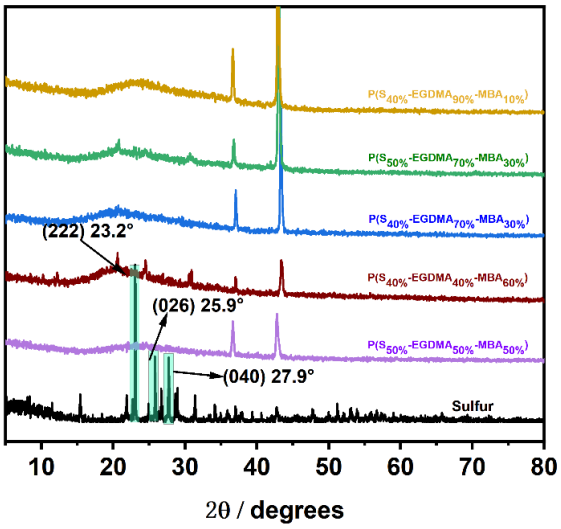

Fig. S32 XRD patterns of poly(S_x-$EGDMA_y$-MBA_z) and S_8.

The results of X-ray diffraction (XRD) measurements indicate the presence of distinct Bragg reflections, S_8 at 23.2° in the (222) plane, 25.96° in the (026) plane, and 27.9° in the (040) plane. Conversely, the absence of characteristic diffraction peaks of

S_8 in poly(S-EGDMA-MBA) suggests the absence of residual elemental sulfur in the copolymer, indicating an amorphous structure.

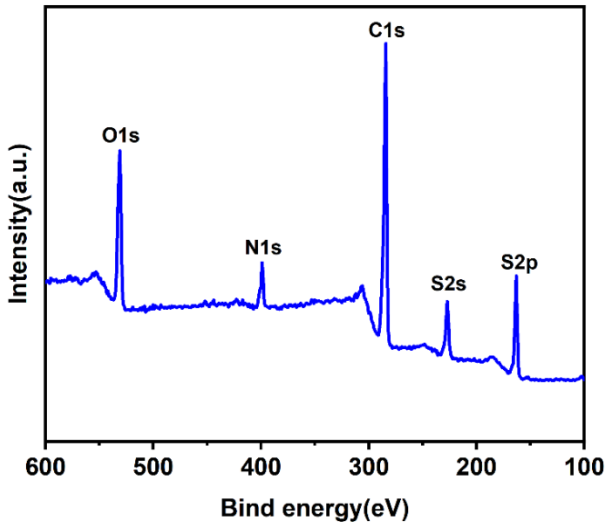

Fig. S33 XPS survey scan of poly(S-EGDMA-MBA).

X-ray photoemission spectroscopy (XPS) is utilized to reveal the bonding modes of various chemical bonds in polymers. The full XPS spectrum can detect C1s, O1s, S2p, S2s, F1s, and N1s orbitals.

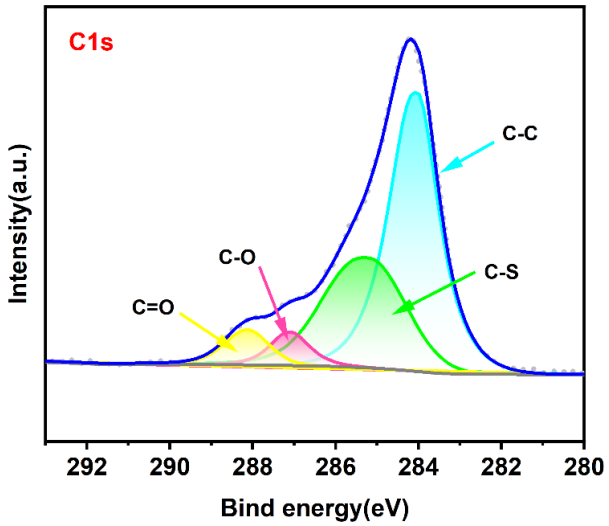

Fig. S34 C 1s XPS of poly(S-EGDMA-MBA)

Its deconvoluted peaks featured for C−O, C−S, C=O, and C−C. High-resolution C1s displays distinct peaks for C-C bonds at 284.2 eV, C-S bonds at 285.33 eV, C-O bonds at 287.2 eV, and C=O bonds at 288.2 eV.

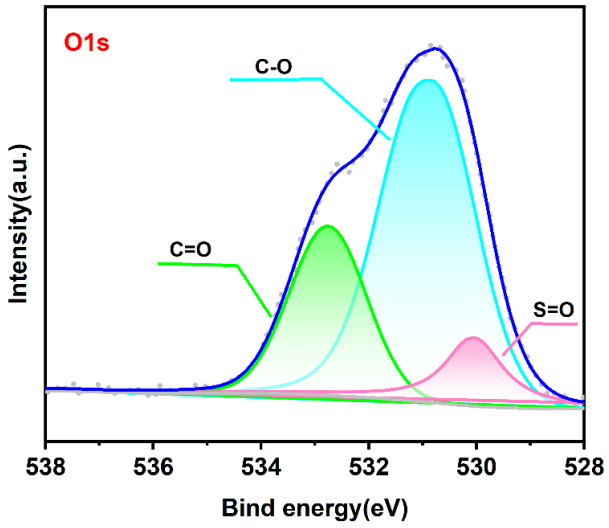

Fig. S35 O 1s XPS of poly(S-EGDMA-MBA)

Its deconvoluted peaks featured for C－O, C=O, and S=O. Similarly, high-resolution O1s exhibits peaks for C-O at 250.2 eV, C=O at 532.8 eV, and C-O at 520.0 eV.

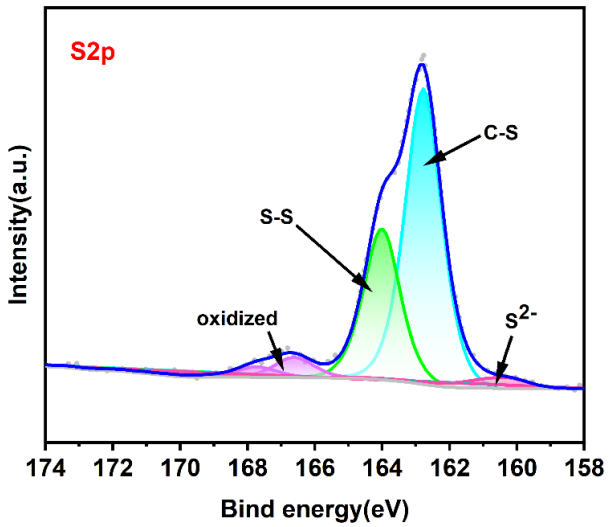

Fig. S36 S 2p XPS of poly(S-EGDMA-MBA)

Its deconvoluted peaks featured for C－S, S-S, S^{2-} and oxidized S. The high-resolution S2p reveals peaks for C-S bonds at 162.8 eV, S-S bonds at 164.0 eV, sulfur oxides at 166.6 and 167.8 eV, and S^{2-} at 160.5 eV.

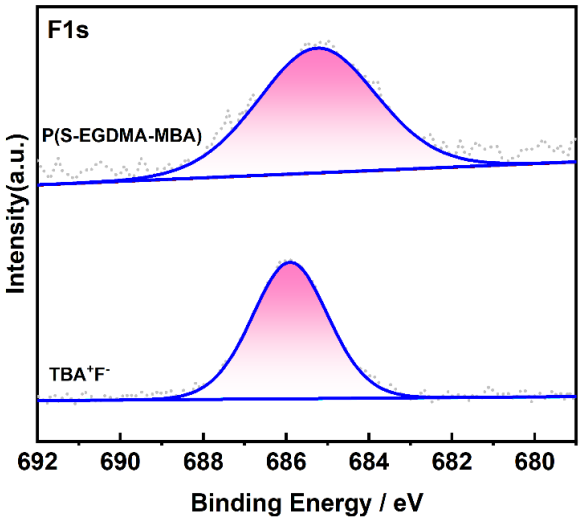

Fig. S37 F 1s XPS of poly(S-EGDMA-MBA)

Comparison of high-resolution F1s between TBAF and the polymer shows the bonding mode of only one of the F in TBAF suggests that F^- is not involved in the reaction and only acts as a source of F for nucleophilic attack to open the S_8.

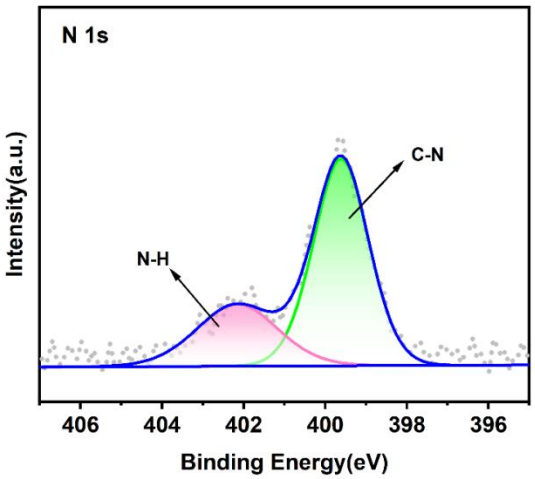

Fig. S38 N 1s XPS of poly(S-EGDMA-MBA)

Its deconvoluted peaks featured for N-H and C-N. High-resolution N1s demonstrates N bonding in N-H and C-N modes. These results demonstrate the successful synthesis of crosslinked copolymers of S_8 with olefins.

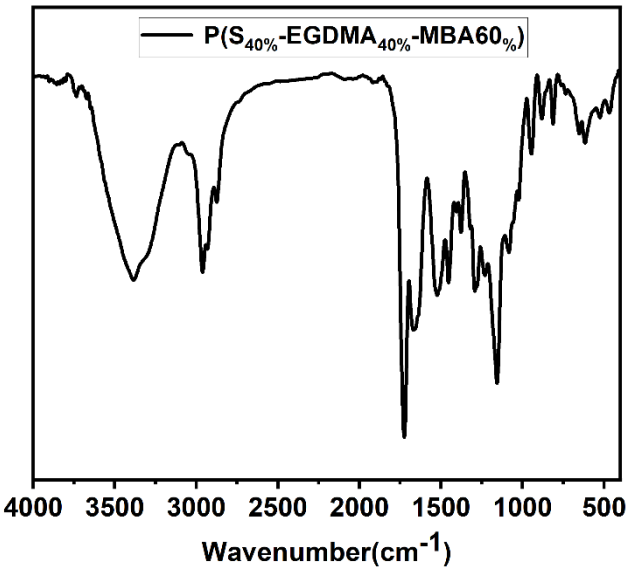

Fig. S39 FTIR spectrum of poly($S_{40\%}$-$EGDMA_{40\%}$-$MBA_{60\%}$).

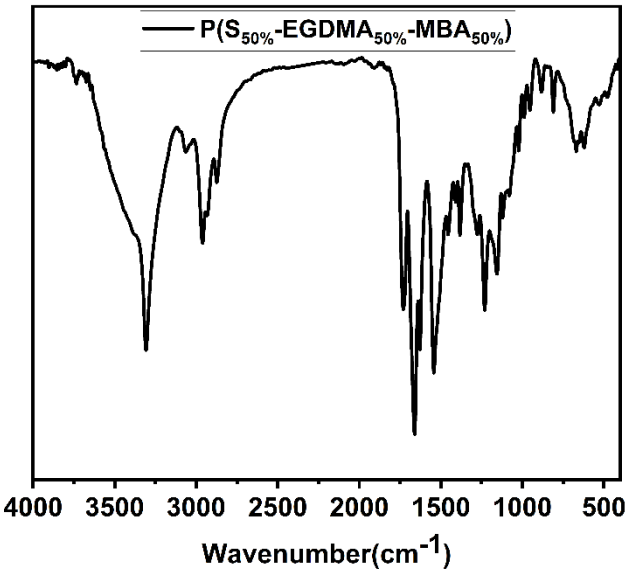

Fig. S40 FTIR spectrum of poly($S_{50\%}$-$EGDMA_{50\%}$-$MBA_{50\%}$).

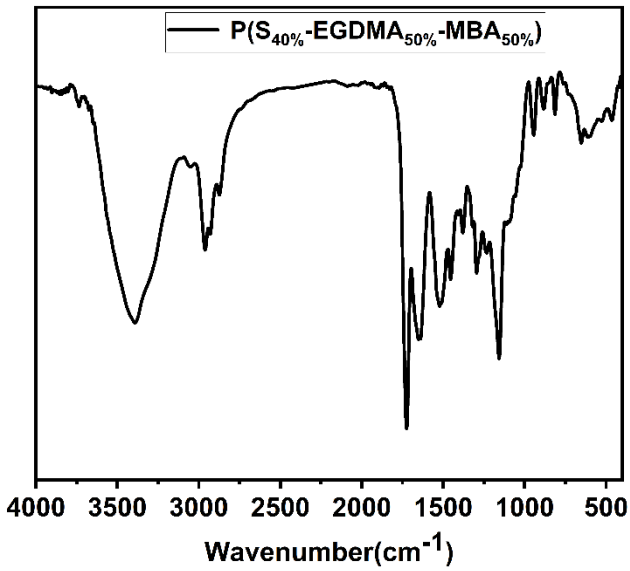

Fig. S41 FTIR spectrum of poly($S_{40\%}$-$EGDMA_{50\%}$-$MBA_{50\%}$).

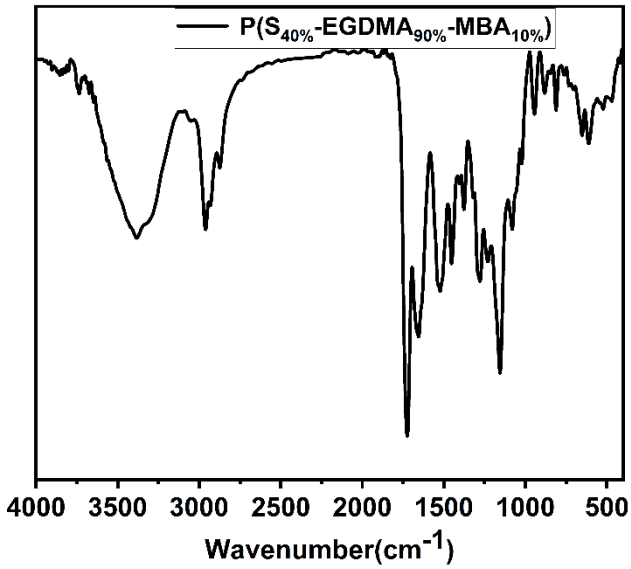

Fig. S42 FTIR spectrum of poly($S_{40\%}$-$EGDMA_{90\%}$-$MBA_{10\%}$).

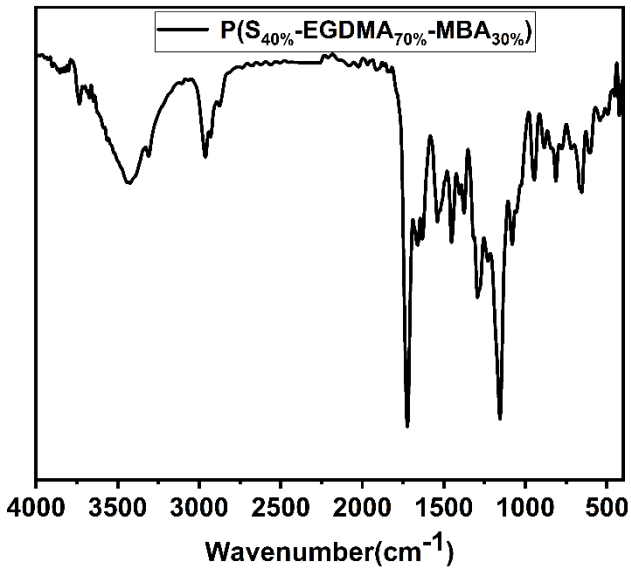

Fig. S43 FTIR spectrum of poly($S_{40\%}$-$EGDMA_{70\%}$-$MBA_{30\%}$).

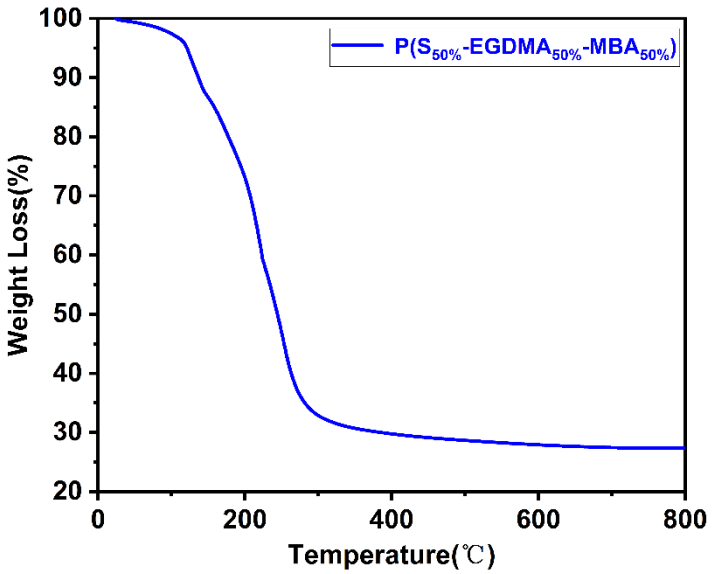

Fig. S44 TGA curves of poly($S_{50\%}$-$EGDMA_{50\%}$-$MBA_{50\%}$).

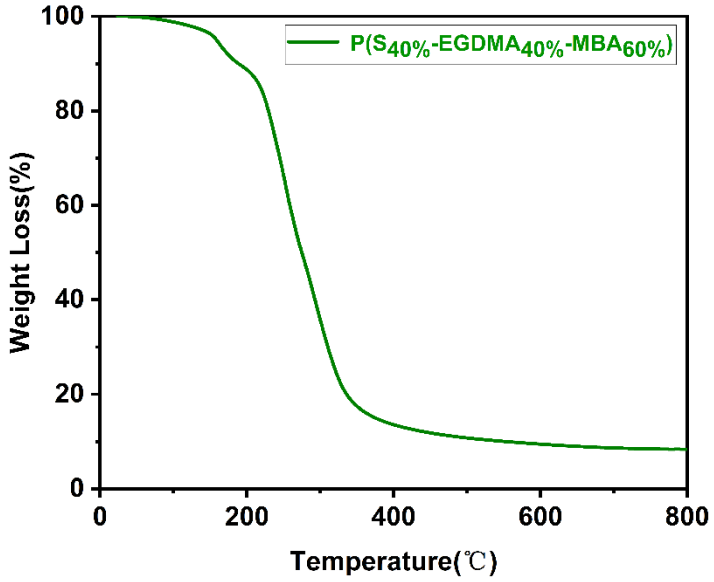

Fig. S45 TGA curves of poly($S_{40\%}$-$EGDMA_{40\%}$-$MBA_{60\%}$).

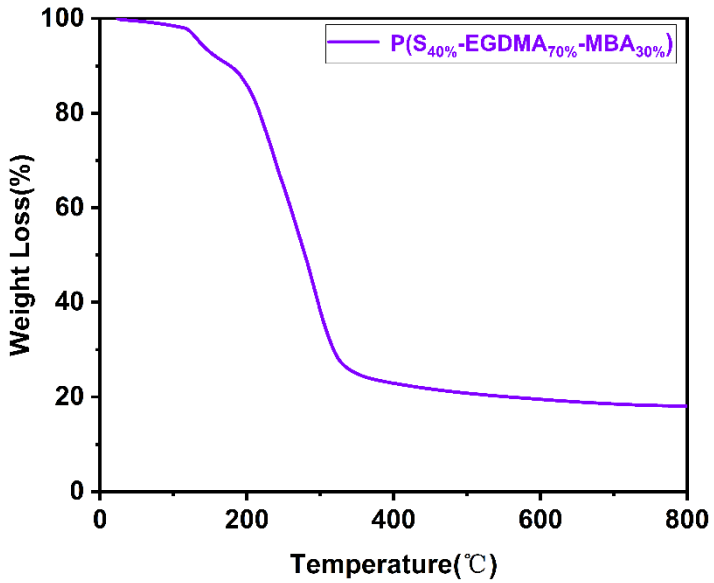

Fig. S46 TGA curves of poly($S_{40\%}$-$EGDMA_{70\%}$-$MBA_{30\%}$).

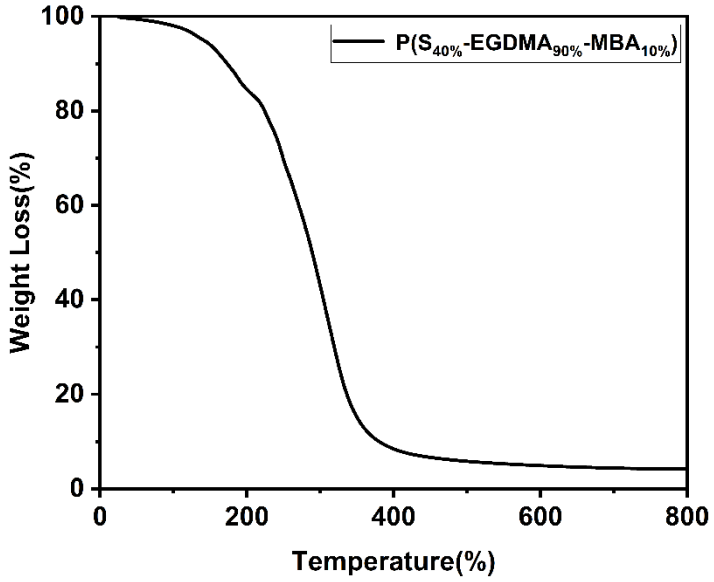

Fig. S47 TGA curves of poly($S_{40\%}$-$EGDMA_{90\%}$-$MBA_{10\%}$).

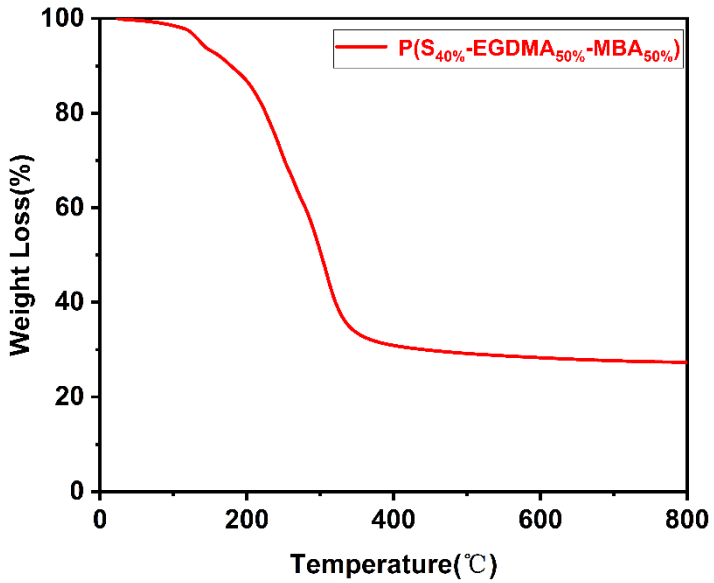

Fig. S48 TGA curves of poly($S_{40\%}$-$EGDMA_{50\%}$-$MBA_{50\%}$).

8. Polymer Solubility Testing

Fig. S49 Solubility determination of poly(S-EGDMA-MBA).

The picture taken within a few minutes after solvents (1.5 mL) were added into the vial contained polymers (5 mg). The results showed that the obtained poly(S-EGDMA-MBA) with r.t. almost have no colour change in all the tested solvents, whereas slightly colour change can be observed with polymers obtained with r.t. in DCM, and completely soluble in DMF. Significant colour change, indicated that the material has high solubility in DMF.

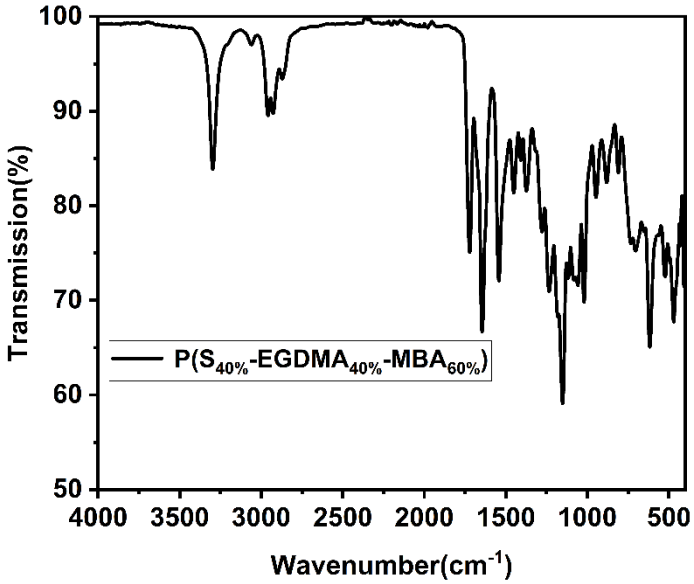

Fig. S50 Average IR transmission spectra of poly($S_{40\%}$-$EGDMA_{40\%}$-$MBA_{60\%}$).

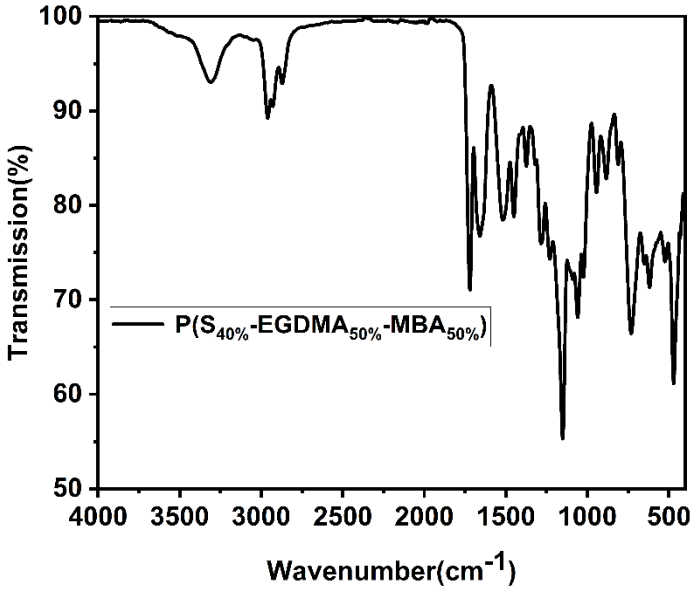

Fig. S51 Average IR transmission spectra of poly($S_{40\%}$-$EGDMA_{50\%}$-$MBA_{50\%}$).

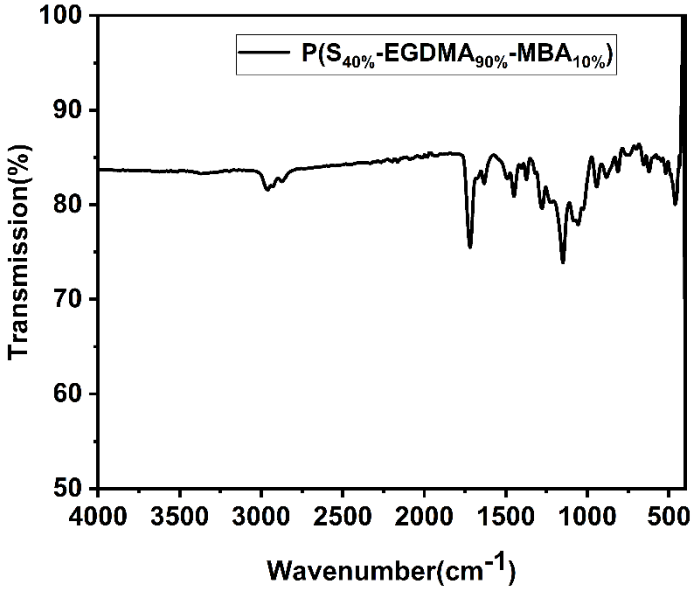

Fig. S52 Average IR transmission spectra of poly($S_{40\%}$-$EGDMA_{90\%}$-$MBA_{10\%}$).

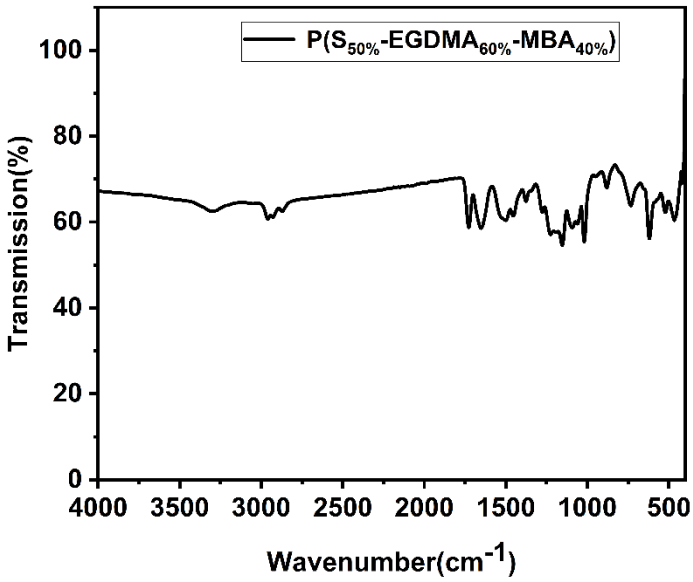

Fig. S53 Average IR transmission spectra of poly($S_{40\%}$-$EGDMA_{90\%}$-$MBA_{10\%}$).

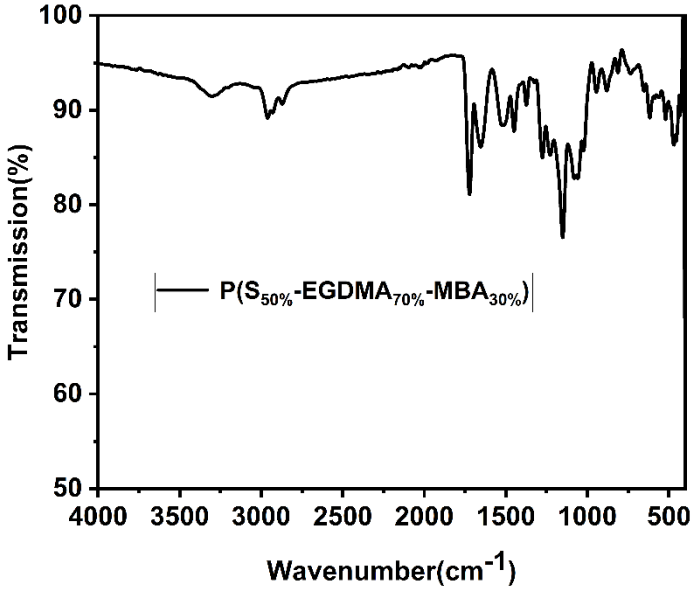

Fig. S54 Average IR transmission spectra of poly($S_{40\%}$-$EGDMA_{90\%}$-$MBA_{10\%}$).

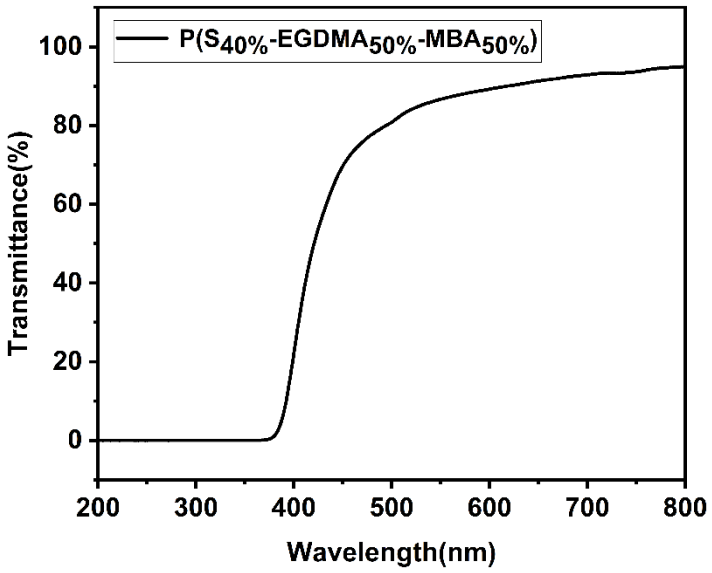

Fig. S55 UV-vis transmittance spectra of poly($S_{40\%}$-$EGDMA_{50\%}$-$MBA_{50\%}$).

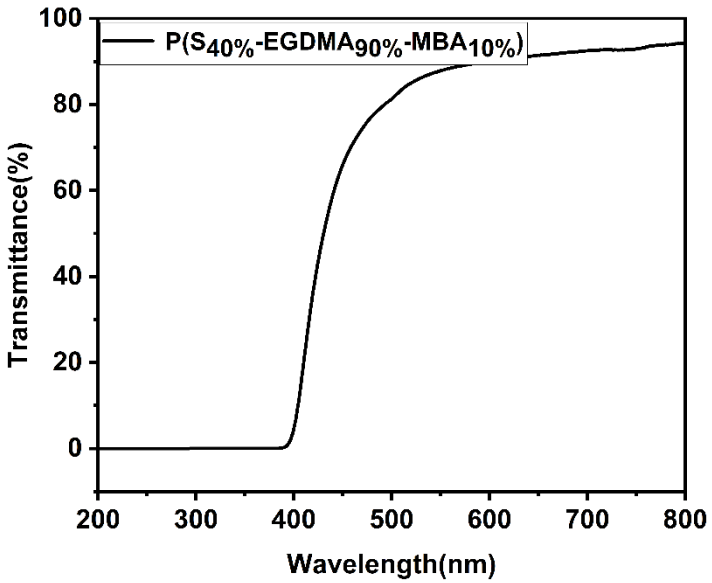

Fig. S56 UV-vis transmittance spectra of poly($S_{40\%}$-$EGDMA_{50\%}$-$MBA_{50\%}$).

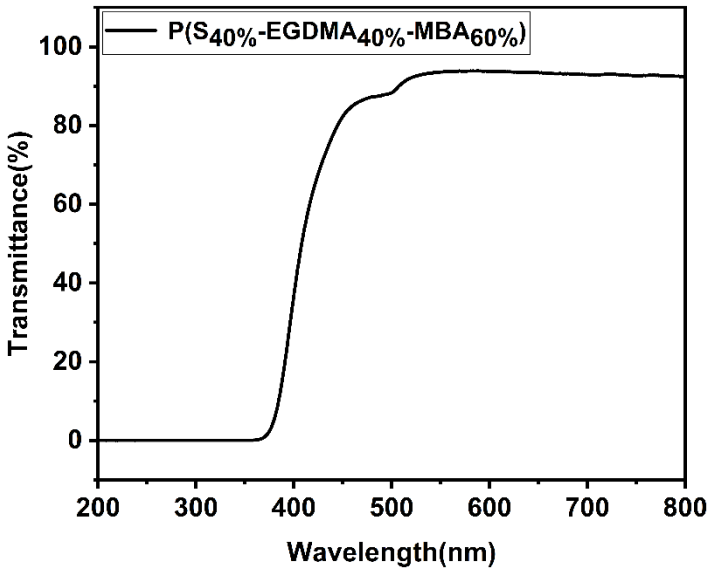

Fig. S57 UV-vis transmittance spectra of poly($S_{40\%}$-$EGDMA_{40\%}$-$MBA_{60\%}$).

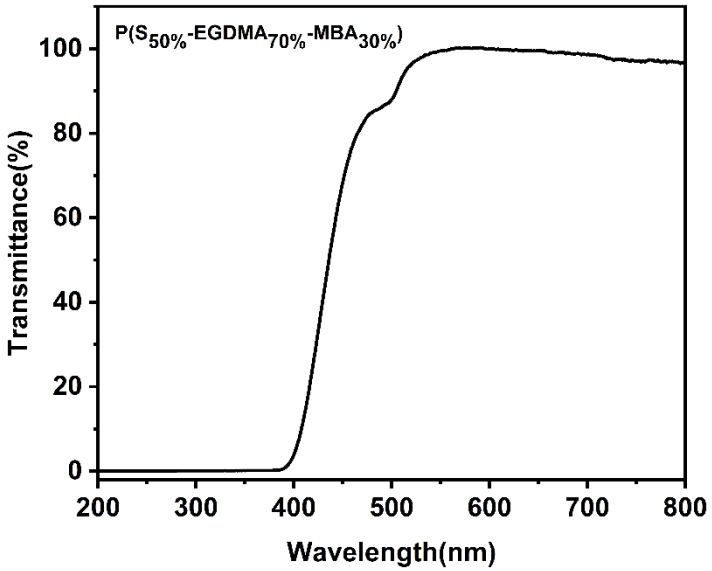

Fig. S58 UV-vis transmittance spectra of poly($S_{40\%}$-$EGDMA_{40\%}$-$MBA_{60\%}$).

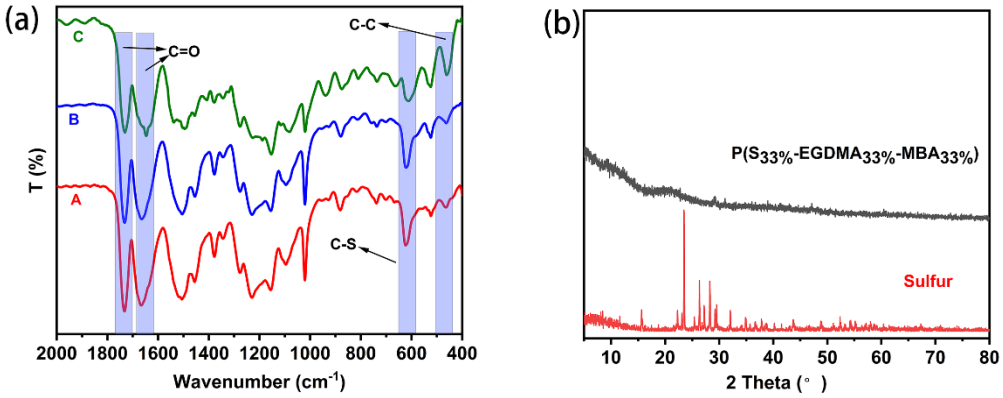

Fig. S59 Stability testing. (a) FTIR of the A (red):P($S_{33\%}$-$EGDMA_{33\%}$-$MBA_{33\%}$), B (blue): P($S_{33\%}$-$EGDMA_{33\%}$-$MBA_{33\%}$) and C (green): P($S_{33\%}$-$EGDMA_{33\%}$-$MBA_{33\%}$) stirring the materials overnight in HCl and NaOH after 6 months of storage, (b) XRD of the P($S_{33\%}$-$EGDMA_{33\%}$-$MBA_{33\%}$) after 6 months of storage.

9. The picture of Poly(S-EGDMA-MBA) polymers with different material ratios.

Fig. S60 The pictures of Poly(S-EGDMA-MBA) polymers with different material

ratios.

10. Pictures of solid products obtained with different crosslinking agents.

Fig. S61 Pictures of solid products obtained with different crosslinking agents.

Picture a is the product obtained from the tube wall during the reaction of poly(S-EGDMA). Where c, d, and e are obtained by verifying the THF dosage, respectively, the THF dosage was 0.3 mL for the c picture, 0.6 mL for the d picture, and 0.9 mL for the e picture.

11. Gel permeation chromatography (GPC) of different polymers

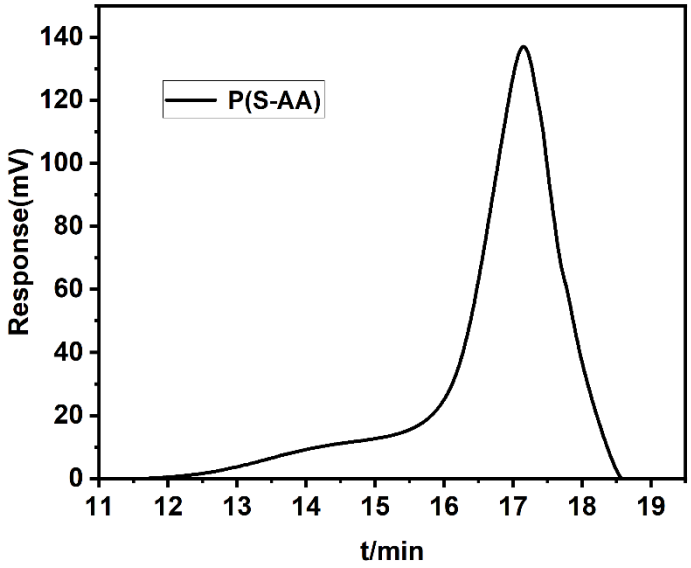

Fig. S62 GPC curve of poly(S-AA) prepared at r.t. 5 mg of polymer dissolved in 1 mL DMF and the mixture was ultrasonic for 1 h before filtrated by syringe with a filtration head (0.22 μm).

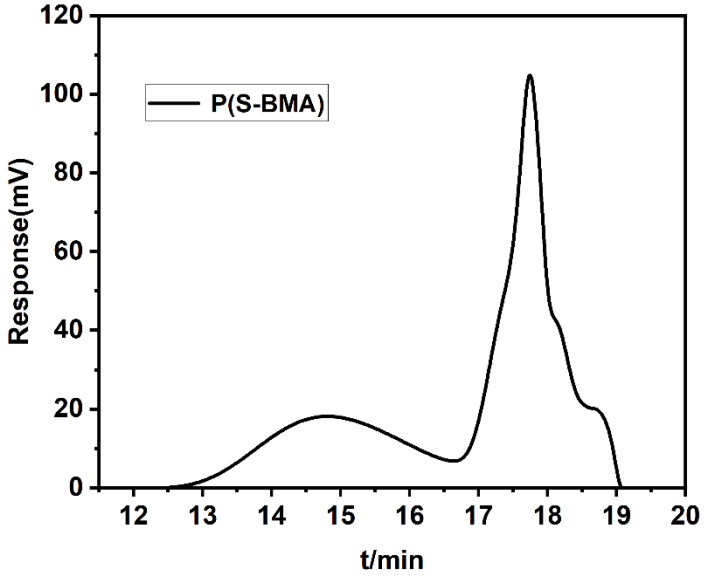

Fig. S63 GPC curve of poly(S-BMA) prepared at r.t. 5 mg of polymer dissolved in 1 mL DMF and the mixture was ultrasonic for 1 h before filtrated by syringe with a filtration head (0.22 μm).

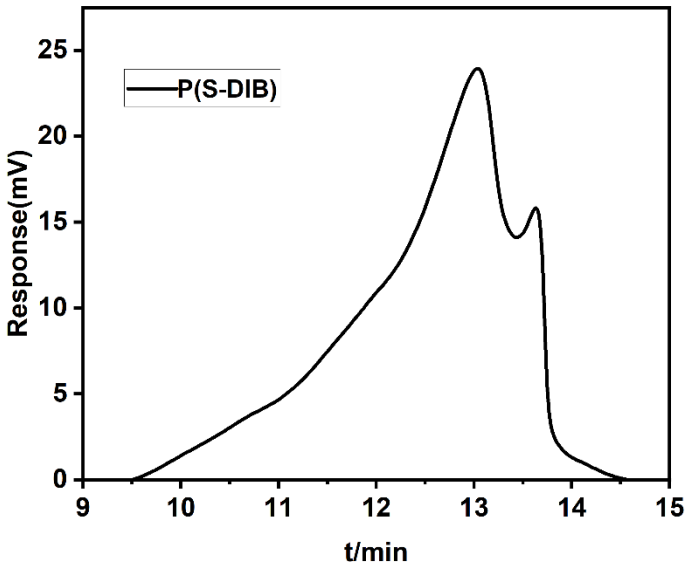

Fig. S64 GPC curve of poly(S-DIB) prepared at 80 ℃. 5 mg of polymer dissolved in 1 mL DMF and the mixture was ultrasonic for 1 h before filtrated by syringe with a filtration head (0.22 μm).

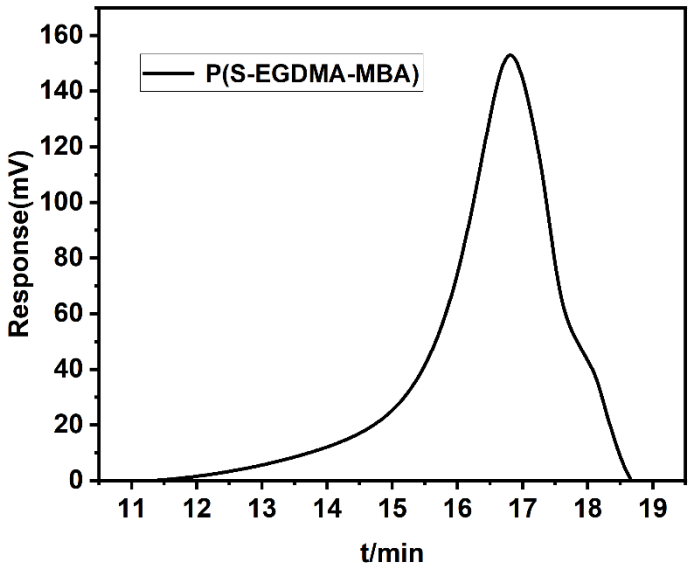

Fig. S65 GPC curve of poly(S-EGDMA-MBA) prepared at r.t. 5 mg of polymer dissolved in 1 mL DMF and the mixture was ultrasonic for 1 h before filtrated by syringe with a filtration head (0.22 μm).

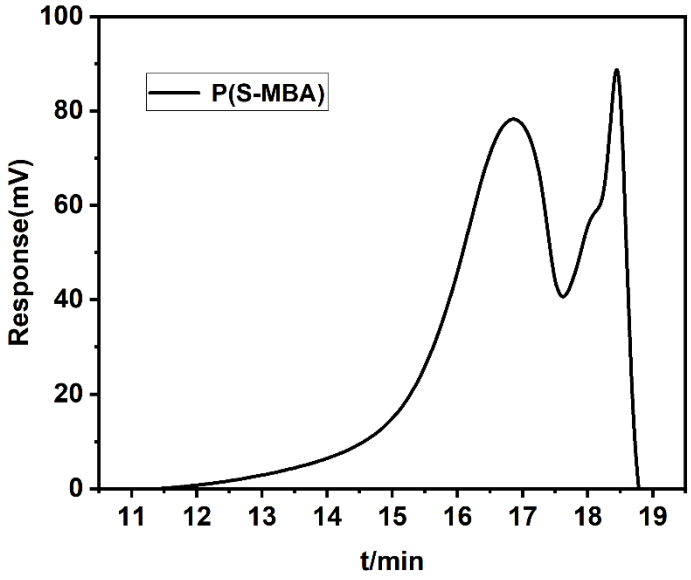

Fig. S66 GPC curve of poly(S-MBA) prepared at r.t. 5 mg of polymer dissolved in 1 mL DMF and the mixture was ultrasonic for 1 h before filtrated by syringe with a filtration head (0.22 μm).

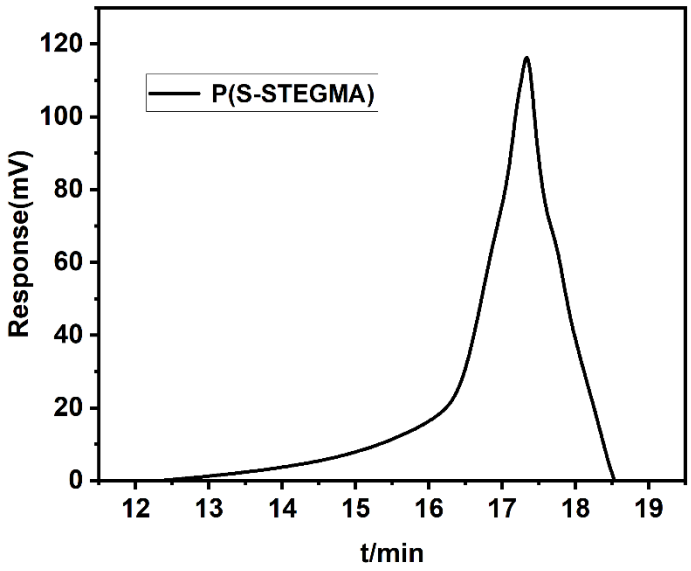

Fig. S67 GPC curve of poly(S-STEGMA) prepared at r.t. 5 mg of polymer dissolved in 1 mL DMF and the mixture was ultrasonic for 1 h before filtrated by syringe with a filtration head (0.22 μm).

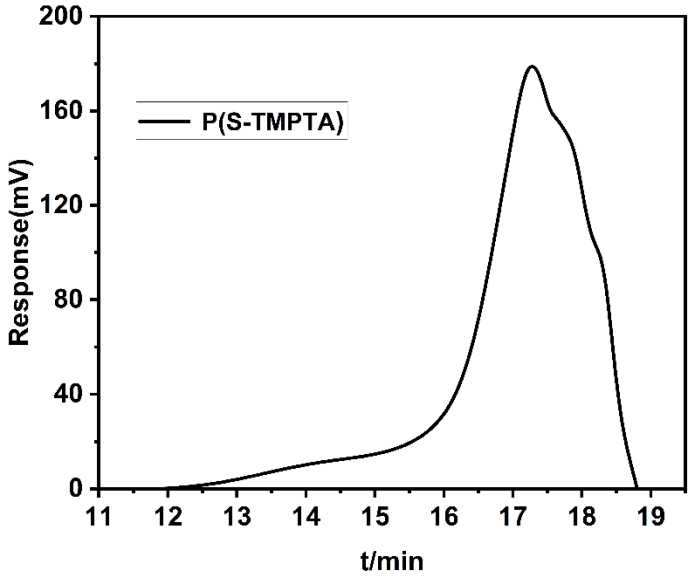

Fig. S68 GPC curve of poly(S-TMPTA) prepared at r.t. 5 mg of polymer dissolved in 1 mL DMF and the mixture was ultrasonic for 1 h before filtrated by syringe with a filtration head (0.22 μm).

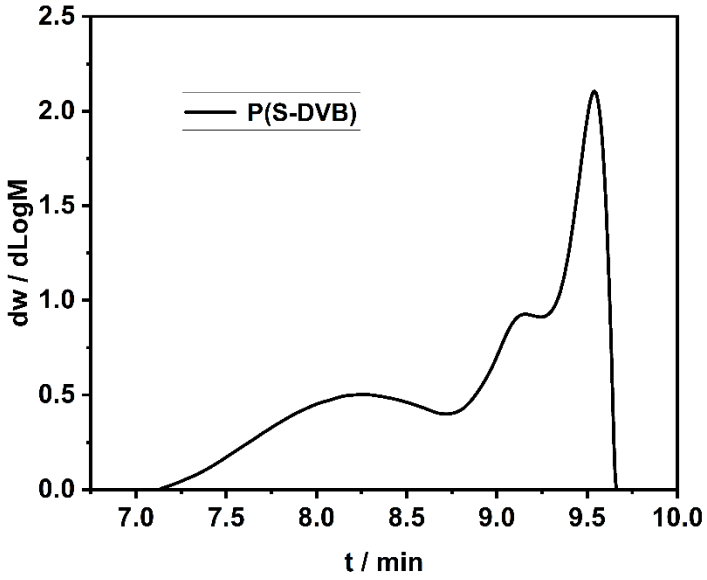

Fig. S69 GPC curve of poly(S-DVB) prepared under 80 ℃. 5 mg of polymer dissolved in 1 mL DMF and the mixture was ultrasonic for 1 h before filtrated by syringe with a filtration head (0.22 μm).

Table S2. Screening of solvents for inverse vulcanization of sulfur with EGDMA

Entry	Solvent	Yield (%)
1	1,4-dioxane	--
2	DCM	--
3	Toluene	--
4	DMSO	--
5	MeOH	--
6	MeCN	--
7	$CHCl_3$	--
8	2-methylfuran	71
9	2-ethyl furan	83
10	dihydropyran	80
11	tetrahydropyran	87

The reaction was at room temperature for 12 h, with stirring. Weight ratio of cross-linker (EGDMA, 300 mg) and sulfur (300 mg) of 1:1 and 5 wt% catalyst loading.

Table S3 Screening of THF dosage of S_8 with EGDMA.[a]

Entry	THF (mL)	Yield (%)
1	0.3	82
2	0.6	75
3	0.9	80
4	1.2	--
5	1.5	--
6	1.8	--

a The reaction was performed with an S_8 to EGDMA weight ratio of 1:1, using TBAF as the catalyst, and a reaction time of 12 hours.

Table S4 Summary of catalytic inverse vulcanization of elemental sulfur with EGDMA crosslinker under different content of TBAF.[a]

Catalyst	Reaction Temp (℃)	Virtification Time[b]	Color
1 wt %	r.t.	--[c]	--
5 wt %	r.t.	12 h	Yellow solid
1 eq	r.t.	2 h	Yellow solid

a Performed with 1:1 weight ratio of S_8 and EGDMA. b Time passed until the magnetic stirring bar stops rotating. c No polymer production was observed within 48 h.

Table S5 Anionic copolymerization of S_8 with EGDMA、MBA.[a]

Entry	S_8 (%)	EGDMA (%)	MBA (%)	Yield (%)

1	40	50	50	>99
2	50	50	50	>99
3	40	40	60	>99
4	50	60	40	>99
5	40	70	30	>99
6	50	70	30	>99
7	40	90	10	>99

a The reaction was conducted at room temperature using TBAF as the catalyst, with a reaction duration of 18 hours.

Table S6 Anionic copolymerization of S_8 with different vinyl monomers.

Entry	**Crosslinker[a]**	**Vitrification Time**	**Conv (%)[b]**	**Observation**	**Yield (%)[c]**	**M_w (g/mol)[d]**
1	EGDMA	12	>99	Dark brown solid	89	--
2	MBA	18	>99	Brown -yellow solid	84	9400
3	AA	18	>99	Dark solid	51	9768
4	TMPTA	18	>99	Yellow solid	58	6376
5	TAT	2	>99	Brown solid	74	--
6	PBzMA	12	>99	Brown viscous material	--	--
7	STEGMA	18	>99	Red-black solid	73	5056
8	BMA	18	>99	Brown viscous material	--	10530
9	PEG	18	>99	Black viscous material	--	---
10	DIB	18	>99	Dark solid	57	2627
11	DVB	12	>99	Dark solid	74	14949
12	St	12	>99	Black viscous material	--	--
13	MYE	12	>99	Black viscous material	--	--
14	1-OC	12	>99	Black viscous material	--	--

Reaction condition：polymerization initiated by TBAF in THF solution at room temperature; a Material ratios of S_8 ： monomers = 1:1. b Conversion of crosslinkers determined by ^{1}H-NMR; c Yield after polymerization is obtained by weighing the mass of polymer, due to the low degree of cross-linking of some cross-linking agents after polymerization with S_8, the polymer obtained is sticky and therefore it is not possible to weigh the polymerization to obtain the yield after polymerization; d M_w obtained by GPC.

12. Computational details

All the calculations were performed using the Gaussian 09 programs[1]. All of the structures were fully optimized with the M06-2X[2] method and 6-31+G** basis set[3, 4] at 298.15K in gas phase.

M06-2X absolute calculation energies (Hartree)

Geometry	G (M06-2x/6-31+G**)
EGDMA	-3185.2760
S_8	-689.9313
F anion	-99.8252
S_8F^-	-3285.1680
Anion-S_8F-EGDMA	-5350.2693
Anion-S_8F-EGDMA+EGDMA	-4664.9926
Anion-S_8F-EGDMA-EGDMA(P)	-4665.0035
Anion-S_8F-EGDMA+S_8	-7160.3643
Anion-S_8F-EGDMA-S_8(P)	-7160.3764

Cartesian coordinates

M062x/6-31+G** geometries for all the optimized compounds

EGDMA

O	-1.76908300	-0.26049500	-0.00017000
C	-0.56378300	0.50497700	-0.00020100
H	-0.52783200	1.14428000	-0.88705600
H	-0.52773200	1.14422800	0.88669300
C	0.56378800	-0.50497300	-0.00023000
H	0.52774100	-1.14427200	0.88663000
H	0.52782600	-1.14423100	-0.88711800
O	1.76908800	0.26049600	-0.00016700
C	2.90823000	-0.45856100	0.00004400
C	-2.90822800	0.45856100	-0.00002700
O	2.91599200	-1.66831000	0.00018000
O	-2.91599300	1.66831100	0.00007600
C	4.14868000	0.37465100	0.00009200
C	-4.14868000	-0.37465400	0.00006200
C	-4.07658900	-1.70801800	0.00000500
H	-4.98026400	-2.31007300	0.00005900
H	-3.12258700	-2.22250900	-0.00010900
C	4.07658200	1.70801500	0.00006400
H	3.12257800	2.22250100	0.00002600

H	4.98025400	2.31007500	0.00004900
C	-5.42808500	0.41117200	0.00019700
H	-5.48004500	1.06187100	0.87764100
H	-5.48019000	1.06193300	-0.87719200
H	-6.28920400	-0.25938300	0.00024400
C	5.42808400	-0.41117400	0.00008500
H	5.48011900	-1.06191000	0.87749500
H	5.48011500	-1.06189700	-0.87733800
H	6.28920200	0.25938200	0.00008500
S_8			
S	0.96836100	0.30352000	-2.01820300
S	0.96836100	2.11105300	-0.85422900
S	-0.39897500	1.95513900	0.64462700
S	0.48220100	0.91494400	2.22780500
S	-0.48220100	-0.91494400	2.22780500
S	0.39897500	-1.95513900	0.64462700
S	-0.96836100	-2.11105300	-0.85422900
S	-0.96836100	-0.30352000	-2.01820300
S_8F^-			
S	1.43332900	0.28811600	-1.09063000
S	2.32161300	-0.82956100	0.35948400
S	0.15840600	-2.31874100	0.63469000
S	-1.32921400	-1.90040400	-0.70144800
S	-2.71397300	-0.63327100	0.21374100
S	-2.28386000	1.34989300	-0.26684200
S	-0.70091700	1.89560200	0.97330000
S	0.94069600	2.13940500	-0.28085400
F	3.86474900	0.01592900	0.28188400
Anion-S_8F-EGDMA			
S	-1.14772200	-0.10959000	-1.18457500
S	-5.40951200	3.19458600	-0.31121500
S	-3.98472400	1.79847500	-0.49934700
S	-3.79577400	0.88584900	1.39415600
S	-5.06113700	-0.74563600	1.33159300
S	-3.92552200	-2.40807700	0.83986300
S	-3.67401300	-2.31711000	-1.23265000
S	-1.63508800	-2.08146900	-1.53612000
F	-6.78975400	2.35592900	-0.62620700
O	6.58954300	0.56239200	0.05199700
C	5.49435100	-0.33054700	0.25450100
H	5.47425800	-1.08286600	-0.53936100
H	5.60458700	-0.84531000	1.21335800
C	4.25180100	0.53349000	0.22850100
H	4.26840300	1.28183300	1.02632900

H	4.14671300	1.05333400	-0.72817000
O	3.15359100	-0.35860700	0.42026000
C	1.93354100	0.22364500	0.42124000
C	7.80834500	-0.01218500	0.05079600
O	1.77516700	1.42141000	0.26523400
O	7.96896700	-1.19990100	0.21482600
C	0.84929500	-0.72865900	0.63294700
C	8.92967200	0.95003100	-0.17097800
C	8.68793900	2.25001600	-0.35740400
H	9.50541300	2.94593500	-0.52023600
H	7.67810800	2.64380900	-0.35222600
C	-0.52018800	-0.17819800	0.56743000
H	-1.23786400	-0.75458500	1.15343900
C	10.29614300	0.32786100	-0.16548600
H	10.48907400	-0.16932500	0.78929500
H	10.37276400	-0.43971100	-0.94068800
H	11.06260700	1.08601400	-0.33536300
C	1.10319800	-2.19180000	0.74799600
H	1.25201000	-2.64129600	-0.24487800
H	2.01157400	-2.38930000	1.32191900
H	0.25386800	-2.69897700	1.21174400
H	-0.54055800	0.87036200	0.87763500
Anion-S_8F-EGDMA+EGDMA			
S	-3.03417000	-1.33301600	-1.38639200
S	-3.70220700	1.74267700	-2.02943100
S	-5.48200100	1.66832100	-1.14509100
S	-5.10081700	1.42792000	0.95267400
S	-6.53288600	0.05776900	1.50743700
S	-5.72749300	-1.84282500	1.67976300
S	-5.84149300	-2.71627800	-0.21466900
S	-3.87595900	-3.10163400	-0.75474100
F	-3.36188200	3.36104200	-1.97061300
O	4.78965300	-0.76697900	-1.21497800
C	3.70056800	-1.44176800	-0.58390900
H	3.74945000	-2.51269600	-0.79483800
H	3.76438400	-1.29683600	0.50034600
C	2.43307800	-0.82314900	-1.13867900
H	2.43345600	0.26688000	-1.04316200
H	2.29082500	-1.06926500	-2.19533300
O	1.37030300	-1.37457900	-0.36101900
C	0.16357000	-0.78494600	-0.52687600
C	5.99050100	-1.37791800	-1.10773200
O	-0.01138700	0.13745000	-1.30971200

O	6.13658600	-2.41815100	-0.50492900
C	-0.87606100	-1.33172200	0.32515600
C	7.10012600	-0.65897200	-1.79626400
C	6.91448000	0.56757700	-2.28976800
H	7.73246700	1.10233800	-2.76318300
H	5.95953200	1.07351000	-2.21025000
C	-2.21229100	-0.71843600	0.16234600
H	-2.87224800	-0.91697000	1.00844200
C	8.40089000	-1.40860400	-1.83391800
H	8.71994100	-1.66938500	-0.82066700
H	8.29266100	-2.34884400	-2.38289600
H	9.17549500	-0.80540200	-2.31122500
C	-0.62496200	-2.37963500	1.34908500
H	0.27776000	-2.95175700	1.13356900
H	-0.49886900	-1.89831700	2.33005300
H	-1.48136200	-3.05733400	1.42478600
O	1.47581800	2.05706300	0.84674500
C	2.43066900	1.25956900	1.54970500
H	2.34472200	1.43677800	2.62567600
H	2.23638600	0.19807100	1.36388700
C	3.78190300	1.68881700	1.01471400
H	3.81426800	1.63863100	-0.07883800
H	4.02573400	2.71238600	1.31256800
O	4.74044700	0.77987200	1.55557600
C	6.01552600	1.01340400	1.17238800
C	0.18528000	1.84647100	1.16369700
O	6.31778700	1.95173200	0.47272000
O	-0.15671900	1.01464300	1.97780000
C	6.95779300	-0.01607300	1.71140600
C	-0.73041000	2.75639500	0.40971200
C	-1.94881500	2.94218000	0.92653400
H	-2.66119800	3.60621800	0.44447100
H	-2.24102100	2.44039300	1.84422700
C	8.24198400	0.11329000	1.36834600
H	8.55964400	0.93020900	0.72768000
H	8.98644700	-0.59570300	1.71747300
C	-0.22103700	3.40337500	-0.84510200
H	0.65166000	4.02779500	-0.63412600
H	0.08666400	2.63385900	-1.56021100
H	-1.00294800	4.01755900	-1.29436500
C	6.41207300	-1.12288900	2.56798600
H	5.85472400	-0.72554600	3.42055300
H	5.73293800	-1.75610000	1.98855100
H	7.22742300	-1.74881800	2.93551200

H	-2.13869000	0.36181500	0.00344100
Anion-S_8F-EGDMA-EGDMA(P)			
S	1.07508800	3.22011500	0.70767100
S	-4.29265100	1.22591200	2.26945500
S	-2.75968100	2.20912900	1.45751100
S	-2.67768400	1.57448200	-0.55850900
S	-3.36892400	3.22154300	-1.60235700
S	-1.73330100	4.24809100	-2.34343500
S	-1.00880200	5.41653300	-0.75731200
S	0.97184100	4.86361800	-0.53173400
F	-5.57169900	2.23229200	2.00615800
O	6.84465900	-0.90825600	-0.35776500
C	5.42072000	-0.92782000	-0.45204500
H	5.11519200	-1.43595800	-1.37191800
H	4.99799900	-1.46077100	0.40427400
C	4.98801900	0.52719700	-0.46273900
H	5.26223200	1.02153300	0.47175900
H	5.42646800	1.05521600	-1.31038500
O	3.57027000	0.59993000	-0.65506800
C	2.80675100	0.40976300	0.43706000
C	7.43422400	-2.12071600	-0.33562300
O	3.26545600	0.18619800	1.53171700
O	6.80449900	-3.15122700	-0.40191600
C	1.31970700	0.49847600	0.10073600
C	8.92303800	-2.06797700	-0.22424500
C	9.56145300	-0.89830100	-0.13875200
H	10.64357000	-0.86439500	-0.05581900
H	9.02253900	0.04202000	-0.14813600
C	1.01693800	1.86908300	-0.53445800
H	1.74210700	2.09118900	-1.31994500
C	9.59555400	-3.41036300	-0.21478400
H	9.23364700	-4.01591200	0.62084100
H	9.36277500	-3.96426500	-1.12856400
H	10.67767500	-3.29574700	-0.13154300
C	0.97694600	-0.56642100	-0.95819300
H	1.46821500	-0.33953500	-1.90701200
H	1.29390400	-1.56422000	-0.63798600
H	-0.10705600	-0.58283600	-1.11171400
O	-1.27297400	-2.92869800	1.79457500
C	-2.55465800	-3.49344400	1.51065400
H	-2.62504700	-4.38769600	2.13159900
H	-3.34499400	-2.78785000	1.77768500
C	-2.63857200	-3.85610300	0.03843300

H	-2.58885900	-2.96539700	-0.59349000
H	-1.83278400	-4.53966300	-0.24569500
O	-3.90218400	-4.50017700	-0.13142600
C	-4.17086700	-4.92314600	-1.38385800
C	-1.11267100	-1.62334700	1.47486400
O	-3.39460800	-4.78133600	-2.29911600
O	-2.01406400	-0.96081100	0.97442000
C	-5.51794400	-5.57105900	-1.47171500
C	0.21310500	-1.10974400	1.78265400
C	0.47882700	0.30754000	1.39324300
H	-0.48249900	0.79738600	1.23065300
H	0.99008200	0.81707000	2.21863000
C	-5.88367600	-6.03881200	-2.66709800
H	-5.21988600	-5.94269900	-3.51997900
H	-6.84599600	-6.52037800	-2.80929600
C	1.25789700	-1.96249100	2.41504700
H	0.81912100	-2.81038700	2.94134100
H	1.94656600	-2.36335700	1.65600000
H	1.87446200	-1.36597900	3.09197500
C	-6.36101900	-5.65139900	-0.23010300
H	-5.84697200	-6.21095000	0.55661600
H	-6.56547900	-4.65373200	0.16867000
H	-7.31024600	-6.14409300	-0.44925200
H	0.01333800	1.83951000	-0.96322500
Anion-S_8F-EGDMA+S_8			
S	0.76912200	1.75803200	0.76291100
S	0.72221000	4.71656000	-0.44119500
S	2.57748500	5.22175300	0.08587700
S	3.88843800	4.17838600	-1.23066100
S	5.28620400	3.37091500	0.05491700
S	4.85566900	1.39712600	0.47426800
S	3.76114400	1.45304300	2.25601700
S	1.95483600	0.50039600	1.87755700
F	0.37157100	5.86296000	-1.58249100
O	4.92368200	-4.12807900	0.11667600
C	3.83703200	-3.60974300	-0.67441200
H	4.22046700	-2.91773700	-1.42536300
H	3.31268100	-4.44065700	-1.15345200
C	2.95575400	-2.91164300	0.35034600
H	2.50815000	-3.64240700	1.02490200
H	3.55226300	-2.18566800	0.91502200
O	1.83877300	-2.23024000	-0.23134400
C	2.08586400	-1.07731500	-0.83956800

C	6.01030400	-4.53335000	-0.54975100
O	3.19780700	-0.65183000	-1.06779400
O	6.14391400	-4.44138700	-1.74855900
C	0.83000000	-0.29999400	-1.27212200
C	7.07054700	-5.11438300	0.33862900
C	6.87797900	-5.23659900	1.65372400
H	7.64854000	-5.66415700	2.28911600
H	5.95094900	-4.91858700	2.11648700
C	1.05180000	1.19085600	-0.96182000
H	2.06038000	1.47328700	-1.27588700
C	8.31810400	-5.54056500	-0.37984800
H	8.08261500	-6.29070900	-1.14006300
H	8.76657000	-4.69313900	-0.90630200
H	9.04484800	-5.95419400	0.32268800
C	0.71658000	-0.43837300	-2.79815600
H	0.62355700	-1.48932700	-3.08221800
H	-0.16454600	0.10372400	-3.15277300
H	1.61703700	-0.02953100	-3.26843600
H	0.32474400	1.78461700	-1.52505000
S	2.24617295	-5.00844947	-5.73263721
S	1.16950918	-3.15831344	-5.53312516
S	2.38557221	-1.74853504	-4.71202740
S	3.55347556	-0.92477395	-6.23595263
S	5.45518056	-1.64639340	-5.85999328
S	5.39638323	-3.61888953	-6.54609198
S	5.45107944	-4.85643716	-4.93179002
S	3.47252857	-5.06214800	-4.11629633
Anion-S_8F-EGDMA-S_8(P)			
S	3.01773300	-0.18546200	-1.80358300
S	5.52234000	-1.82744000	-0.50680900
S	6.28427400	-0.31272800	0.53543400
S	4.92747800	0.05542700	2.14796800
S	4.77855500	2.11071800	2.14535900
S	3.09018200	2.72876600	1.12915100
S	3.70070200	2.96383900	-0.86446000
S	2.40594700	1.77885300	-1.95812600
F	6.14970800	-3.13812700	0.27310500
O	-3.21305200	3.42867500	-0.55241300
C	-2.56045200	2.16188500	-0.49543700
H	-2.35894900	1.89447700	0.54549800
H	-3.20081000	1.39309100	-0.94248400
C	-1.26819000	2.28874200	-1.27792900
H	-1.45578800	2.59056100	-2.30884900

H	-0.57205900	2.98171300	-0.79832600
O	-0.67852500	0.98566700	-1.36187400
C	0.00319400	0.57418500	-0.29001700
C	-4.37436800	3.48413100	0.12908600
O	0.15893800	1.23392800	0.70986000
O	-4.81426600	2.53368300	0.73714500
C	0.57197600	-0.84808100	-0.40589400
C	-5.05777500	4.80973100	0.06456900
C	-4.52039800	5.82121700	-0.62192400
H	-5.01907400	6.78463800	-0.66736800
H	-3.57928600	5.71055700	-1.14810500
C	2.10752300	-0.78294800	-0.33127400
H	2.38753200	-0.18168100	0.53859900
C	-6.35396500	4.88160800	0.81881400
H	-7.06104700	4.13808200	0.44051600
H	-6.19631200	4.65645600	1.87730200
H	-6.79568000	5.87525200	0.72641900
C	0.08635700	-1.62124600	0.82744500
H	-1.00584400	-1.64788100	0.86425900
H	0.45693900	-2.64854500	0.79568900
H	0.44460700	-1.12276400	1.73208800
H	2.50162500	-1.79413000	-0.18348300
S	-3.95107200	-3.86103300	1.38599000
S	-3.50898300	-2.22513400	2.49675900
S	-3.99125300	-0.47853900	1.25273400
S	-5.00846100	-1.05071200	-0.28544200
S	0.12750400	-1.68565900	-1.98648600
S	-1.93864600	-1.76952600	-1.82737600
S	-2.45359000	-3.77184500	-1.62081000
S	-2.21029600	-4.37313300	0.34119200

References

1 M. J. Frisch, G. W. Trucks, H. B. Schlegel, G. E. Scuseria, M. A. Robb, J. R. Cheeseman, G. Scalmani, V. Barone, B. Mennucci, G. A. Petersson, H. Nakatsuji, M. Caricato, X. Li, H. P. Hratchian, A. F. Izmaylov, J. Bloino, G. Zheng, J. L. Sonnenberg, M. Hada, M. Ehara, K. Toyota, R. Fukuda, J. Hasegawa, M. Ishida, T. Nakajima, Y. Honda, O. Kitao, H. Nakai, T. Vreven, J. A. Montgomery, J. E. Peralta, F. Ogliaro, M. Bearpark, J. J. Heyd, E. Brothers, K. N. Kudin, V. N. Staroverov, R. Kobayashi, J. Normand, K. Raghavachari, A. Rendell, J. C. Burant, S. S. Iyengar, J. Tomasi, M. Cossi, N. Rega, J. M. Millam, M. Klene, J. E. Knox, J. B. Cross, V. Bakken, C. Adamo, J. Jaramillo, R. Gomperts, R. E. Stratmann, O. Yazyev, A. J. Austin, R. Cammi, C. Pomelli, J. W. Ochterski, R. L. Martin, K. Morokuma, V. G. Zakrzewski, G. A. Voth, P. Salvador, J. J. Dannenberg, S. Dapprich, A. D. Daniels, Farkas, J. B. Foresman, J. V. Ortiz, J. Cioslowski and D. J. Fox, 2009.

2 Y. Zhao, D. G. Truhlar, *Theor. Chem. Acc.* **2008,** *120*, 215-241.

3 G. A. Petersson, M. A. Al‐Laham, *The Journal of Chemical Physics* **1991,** *94*, 6081-6090.

4 G. A. Petersson, A. Bennett, T. G. Tensfeldt, M. A. Al‐Laham, W. A. Shirley, J. Mantzaris, *The Journal of Chemical Physics* **1988,** *89*, 2193-2218.